Impact of anthropogenic activities on woodland in northern Syria (4th-2nd mill. BC): Evidence from charcoal assemblages and oak measurements

Katleen Deckers[1], Federico Polisca[2], Simone Riehl[3], Michelle de Gruchy[4], Dan Lawrence[5]

[1] University of Tübingen, Institute for Archaeological Sciences, Hölderlinstraße 12, 72072 Tübingen, Germany. Orcid ID: https://orcid.org/0000-0001-8087-5306 – corresponding author: katleen.deckers@uni-tuebingen.de

[2] University of Padova, Dipartimento dei Beni Culturali, Piazza Capitaniato 7, 35139 Padova, Italy. Orcid ID: https://orcid.org/0000-0002-7381-9987

[3] University of Tübingen and Senckenberg Center for Human Evolution and Palaeoenvironment (HEP), Hölderlinstraße 12, 72072 Tübingen, Germany. Orcid ID: https://orcid.org/0000-0002-1744-0032

[4] Durham University, Department of Archaeology, Department of Archaeology, Durham, United Kingdom. Orcid ID: https://orcid.org/0000-0002-7856-8013

[5] Durham University, Department of Archaeology, Department of Archaeology, Durham, United Kingdom. Orcid ID: https://orcid.org/0000-0001-5613-1243

Keywords

Anthracology – diameter measurements – ring width – Uruk period – Early Bronze Age – Middle Bronze Age -northern Syria – vegetation – herbivore impact

Abstract

In this paper charcoals from the Syrian sites Tell Mozan and Tell Jerablus are investigated to understand the impact of 4th to 2nd millennium BC settlement and urbanization on the vegetation. In total 18,786 charcoal fragments from these sites have been identified and additionally oak charcoals have been measured for their maximal diameter and annual ring widths. Our results show that while oak had reached its maximal expansion in the Mid-Holocene, and vegetation in the Euphrates Valley was lusher than today, strong anthropogenic impact on the vegetation was occurring, probably already prior to the Late Chalcolithic period. Due to potentially enormous herds of sheep and goat, and possibly large-scale agriculture with perhaps some understory cropping, oak was growing very slowly, to the degree that it must often have had a shrub-like appearance. People did not apply systematic oak woodland management practices, such as coppicing or pollarding. They used dung as an additional fuel, probably to cover for shortages in wood resources. The land appears to have been used both intensively and extensively to a degree that was not sustainable in the long term, especially in the Early Bronze Age. Overgrazing and unsustainable agricultural practices increased desertification and made the political, settlement and provisioning systems vulnerable to collapse. This, combined with aridity impact on the oak, probably led to a decrease in oak proportion

at Mozan in the Middle Bronze Age, which matches with the contemporary regional increase in desert-steppe environments observed from the seed data.

Introduction

Anthracology plays a key role in the reconstruction of woody vegetation in much of the Near East, since palynological research is hampered by poor pollen preservation. The discipline has traditionally focused on the identification of species and taxa recovered from excavation contexts at archaeological sites to investigate wood use and vegetation development. More recently, several new methods have been introduced which allow for the extraction of additional archaeological and palaeoenvironmental information. One of these is wood diameter analysis, a technique which can identify which parts of the tree have been used, enabling the reconstruction of firewood use and management, and practices such as coppicing (cutting down to near ground level to grow new shoots), pollarding (cutting to the main stem or trunk encouraging lateral branches) and woodland clearance (Dufraisse 2006; Kabukcu 2018; Salavert and Dufraisse 2014; Wright 2018). In combination with annual ring-width data, diameter analysis can also provide information on the structure and appearance of the woodland and the environmental conditions trees experienced during their lifetime (Deckers 2016; Nelle 2002).

Most of Syria, especially also our research area, is geobotanically classified as associations of Mesopotamian steppes of *Artemisietea herbae-albae mesopotamica* (Zohary 1973). The modern landscape of northeastern Syria is largely devoid of woodland, although small stands of *Populus euphratica* (Euphrates poplar), *Salix acmophylla* (weeping willow), and *Tamarix tetrandra* or *T. smyrnensis* (tamarisk) are found along the Euphrates River valley and major tributaries such as the Khabur. Outside of the river valleys, most of the landscape is given over to dry farming of wheat and barley (Shafer and Blomo 1980: 32), and after harvesting in the summer plant life is very limited. Interannual variability in rainfall in this region is high and the limit of dry-land farming (often represented by the 250 mm isohyet, although this should not be taken as a hard border) has shifted regularly to the north upon low rainfall and to the south upon high rainfall (Wilkinson 1997, Hewett et al. submitted). Over the last decades, the area has received progressively less rainfall, in comparison with long-term averages (compare Hewett et al. submitted with data from between 1961-1990 with www.worldweatheronline.com).

Anthracological research indicates that the landscape looked somewhat different in the Mid-Holocene (ca. 6200-2200 BC), with deciduous oak having a more southward distribution and riverine vegetation being lusher (e.g., Charles et al. 2010; Deckers, 2010; Deckers & Riehl, 2007; Deckers & Pessin, 2010; Engel 1993; Pessin 2004, 2007; Willcox 1999). This was probably favored by moister conditions during the Mid Holocene than today (Wick et al. 2003). Also during the Mid-Holocene (ca. 6200-2200 BC) the region went through the first of two phases of urbanization, initially in the fourth millennium BC, followed by a second iteration in the mid-late 3rd millennium BC (Ur 2010a; Wilkinson et al. 2014; Lawrence et al. 2021). The first phase in the Late Chalcolithic (4400 to 3000 BC) is marked by population agglomeration in some areas (especially in the Upper Khabur Basin, but also visible to a lesser degree in other fertile plains), specialized craft production (including mass production of ceramics), monumental architecture, long-distance trade, religious institutions and large-scale feasting, but there is no evidence for writing at that time in northern Syria (Ur 2010a; Wilkinson et al. 2014). This phase then was followed by a phase of population and urban stability, before the second urbanization peak (Palmisano et al. 2021).

From 2600 BC onward a second wave of urbanization occurred, representing “the most pervasive phase of urban settlement prior to the 20th century AD“ (Ur 2010a: 404). It was marked by a three to four-tiered settlement hierarchy, and the urban centers included massive city walls, palaces and temples. There is evidence for increased specialization and intensification in the pastoral sector (Ur 2010a; Gaastra et al. 2020; Gaastra et al. 2021; Price et al. 2017), with dung being increasingly used as (additional) fuel at Middle Euphrates sites, especially those further south, suggesting decreased availability of woody resources (Miller 1997). Writing is used for the first time during this phase, specifically in the realm of the palace and its economic administration (Kolinski 2007). The texts indicate that specialist pastoralists were a significant part of the political economy (Arbuckle and Hammer 2019), with city states managing huge holdings of e.g., sheep and evidence for intensive textile and meat production (Milano 1995; Archi 1993; Sallaberger 2004). Additionally, based on lower $\delta^{15}N$ values of seeds and a lack of change in the $\delta^{13}C$ values, it has been argued that extensification instead of intensification took place within the agricultural sector. This would have consisted of the expansion of the agricultural land to produce more harvest instead of increasing energy input per unit area, for example through manuring or irrigation, to achieve a larger harvest (Styring et al. 2017). The presence of intensive off-site sherd scatters surrounding the settlements, however, indicates that manuring nonetheless took place (Wilkinson 1989). Pastoralism and agricultural extensification in combination with population increase would likely have impacted the scale of agricultural and pastoral land use, and therefore the survival of woodland.

After the second wave of urbanization, settlement disruptions took place in northern Mesopotamia at the end of the 3rd millennium BC (2200-2000 BC). Climatic drying may have played a role in this (Staubwasser and Weiss 2006; Weiss et al. 1993), perhaps also in combination with unsustainable land use practices (Wilkinson 1997; Lawrence et al. 2021). In the Upper Khabur Basin, many sites were abandoned, but in the Middle Euphrates settlement change is more limited. In fact, it has even been argued that the latter region may have received refugees from other areas (Burke 2014). In the second millennium BC the Eastern Upper Khabur region was repopulated, but settlement was more uneven, with fewer urban centers. The texts of that period indicate that the landscape was used for agriculture and pasture (Ristvet 2007).

We would thus expect to see a strong impact of urban societies on vegetation, especially during the second wave of urbanization, combined with climatic impact on vegetation towards the end of the 3rd millennium BC. Anthracology can help in understanding land use, climate and their impact on the vegetation. Here we describe the results of charcoal identifications, of wood diameter analysis and annual ring width measurements on charcoal samples from two sites in northern Syria, Tell Jerablus Tahtani and Tell Mozan. Both sites are well-studied multiperiod sites, which allows us to investigate changes over time. Both sites also were located within the southward distribution of oak, which allows us to compare data for oak (Deckers 2016). Additionally, we purposely selected a small (Jerablus) and a large (Mozan) site (Peltenburg 1999 and Pfälzner 2010) to understand possible differences between the impact of small and large sites on the vegetation. We compare our data with available data from other sites in the region. The goal is to understand how woodland resources were managed, whether there is evidence for unsustainable land-use, and whether we can identify the impact of aridification. This allows us to contribute to the question of the organization of Bronze Age centers and their impact on the environment.

The sites

Tell Jerablus is a multiperiod tell site, located on the right bank of the Euphrates River in northern Syria, about 4 km south of the Turkish border (Fig. 1). It received a long-term average annual rainfall of 458 mm between 1961-1990 (Hewett et al. submitted). Excavations took place at the site under the direction of Edgar Peltenburg and 5 major occupation periods could be identified between the later part of the Late Chalcolithic (from ca. 3600 BC onwards) and Islamic period (13th century AD) (Peltenburg 1999). Here we focus on Periods I and II, respectively the Late Chalcolithic/Uruk and the Early Bronze Age. The site was founded in the 4th millennium BC (Period IA) before the Uruk period.

The pre-Uruk settlement evidence consists of pits, middens, mudbrick walls, postholes, hearths and surfaces, but no coherent architectural insight could be gained. Directly above the Late Chalcolithic levels, Uruk period occupation was found (Period IB, dated to ca. 3500-3000 BC) (Peltenburg and Wilkinson 2008). As in other areas (Algaze 2008), the Uruk period is marked by a sudden intrusion of southern Mesopotamian material culture, suggesting Jerablus may then have been an Uruk colony or an enclave. This occupation ends abruptly but there is no evidence for destruction (Peltenburg and Wilkinson 2008). After the Uruk phase an open Early Bronze Age settlement was built over an area of ca. 12 ha (Period IIA, from ca. 3000 BC onwards) (Wilkinson et al. 2007). There remains evidence for long distance contacts at the site during that period. Subsequently, at about 2825-2720 BC the settlement was destroyed and burnt to ashes. Perhaps as a response to this event, a fortification wall was constructed during the following Period IIB (ca. 2800-2250 BC) and the lower town was abandoned, with settlement (still seemingly domestic in nature) confined to the area surrounded by walls. The construction of the fortifications and the arrangement of houses within the walls were all part of a single plan, and the scale of the fortifications suggest a central administration capable of mobilizing a significant amount of labor. It has been suggested this power was the nearby urban center at Carchemish, only about 4 km to the North (Peltenburg 2016). Alternatively, it may have been an autonomous initiative, related to internal upheaval and site-based authority (Peltenburg 2016). Similar fortifications are known from several other small tells during this period and may be part of a pattern of fortifying even very small sites (Lawrence and Rey 2020). Jerablus was not itself a large urban center at this time, but possibly rather a kind of outpost, perhaps to control riverine traffic or pastoralists. Soon after the construction of the fortifications, probably around 2500 BC (still Period IIB), a glacis was built, and the entire structure was artificially raised. From that period, granary structures and evidence for textile, metal production and crop-processing have been discovered. Based on the overall evidence the excavator suggests this mirrors the intensification of production and increased specialization visible at other sites which has been related with the emergence of city states at that time (Peltenburg 2016). In the case of Jerablus, it is possible that Ebla controlled it, since Ebla claimed control of Carchemish and associated small sites (Lawrence and Rey 2020). Around the mid-3rd millennium BC major flooding of Tell Jerablus and its surroundings took place, but the community persisted. Around 2270-2155 BC the site was abandoned, and it has been suggested that the inhabitants went to the nearby center of Carchemish (Peltenburg 2016).

Tell Mozan is located 250 km east of Jerablus in the Upper Khabur Basin of Syria (Fig. 1) and received on average 434 mm/year over the long-term (Hewett et al. submitted). Investigations of CORONA satellite photographs from the 1960s and geomorphological research indicates that an intermittent stream ran through the western lower town of Mozan probably during the Early Bronze Age (Deckers and Pustovoytov 2011). The site has been excavated under the direction of Giorgio Buccellati, Marilyn Kelly-Buccellati and Peter Pfälzner. Occupation at Mozan dates back to at least the beginning of the fourth millennium BC, but not much is known about the site between the 4th millennium BC and the Early Jezirah II period (EJII) (2750-2600 BC) (Buccellati and Kelly-Buccellati 1999). While the settlement was largely confined to the 15-ha upper town during the EJII (2750-2600 BC), in the Early Jezirah III (EJIII) period (2600-2300 BC) significant settlement expansion took place, extending over an area of 120 ha and protected by a fortification wall. It had several large, monumental buildings and a central plaza, suggesting a complex and structured political system. This was the major phase of urbanization (Pfälzner 2010). Tell Mozan has been identified as the late 3rd millennium Hurrian capital of Urkesh. It was probably an ally or vassal of the Akkadian Empire around 2300 BC (Buccellati and Kelly-Buccellati 1999). From the Early Jezirah IV (EJIV) (2300-2100 BC) through the Early Jezirah V (EJV) period (2100-2000 BC), a gradual population decline took place at the site, especially within the lower town. However, unlike many other sites in this area, Mozan was continually occupied across the end of the 3rd millennium BC. In the Early Jezirah V period domestic dwellings were constructed in the upper city, which may be indicative of a decline in the importance of centralised authority within the city. However, continuation is visible, and a merchant house was built during the Early Jezirah V period (Pfälzner 2010). The continued occupation at the site between 2200 and 1900 BC may correlate with the then newly established kingdoms of Urkesh and Nawar (Buccellati and Kelly-Buccellati 1999). From the Middle Bronze Age onwards (2000 BC) the lower town was abandoned, but several of the existing architectural structures in the upper town continued to be in use, including a merchant house from which a lot of the investigated charcoals derive. Besides that, some new foundations for houses and new street arrangements were laid out, and a new ceramic assemblage appears. This suggests that some new occupants may have arrived at the site about that time, but they did not necessarily replace the population (Pfälzner 2010). During the second millennium BC the city passed to the rulers of Mari and became a vassal (Buccellati and Kelly-Buccellati 1999), before being abandoned about halfway through the second millennium BC (Pfälzner 2010).

Besides our own data from Jerablus and Mozan, our results are compared with anthracological data from Kaman-Kalehöyük (Fig. 1), which is a multi-period site in Turkey, about 500 km away from our sites. We especially compare with second and first millennium BC diameter data from domestic contexts from this site. At that time, Kaman was a modest sized town or large village (Wright 2018).

Additionally, we also compare data with available ring width data from the Euphrates Valley. Earliest comparative evidence derives from Horum Höyük, a Chalcolithic and Early Bronze Age site in Turkey, ca. 40 km north of Jerablus (Pessin 2004), today receiving approximately 510 mm of rainfall annually on average (Hewett et al. submitted) (Fig. 1). Additionally, ring width measurement data is available for Late Bronze Age and Iron Age Tell Shiukh Fawqani, which is located on the opposite bank of the Euphrates to Jerablus (Fig. 1) (Pessin 2004). Exceptional long and well-dated sequences of ring widths are available from the Late Bronze Age to Iron Age site of Tille Höyük, located further north in Turkey on the right bank of the Euphrates, receiving today on average 514 mm rainfall/year (Fig. 1)(Griggs and Manning 2009; Griggs et al. https://www.ncdc.noaa.gov/paleo-search/study/8516, accessed online 09.06.2020, Hewett et al. submitted)

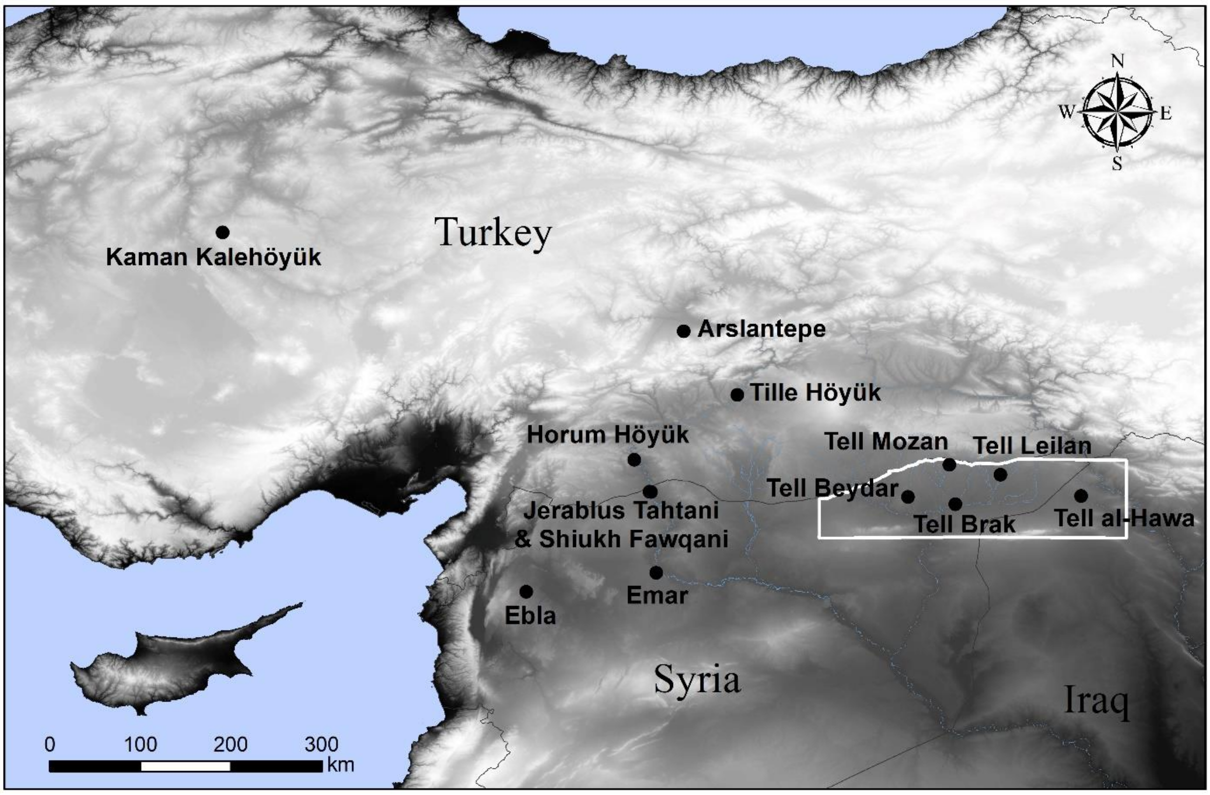

Fig. 1. Map with location of the sites mentioned in the text. The white delineation indicates the area mentioned in Fig. 12.

Materials and methods

In total 242 charcoal samples, consisting of 16 943 identifiable fragments, were analyzed from the archaeological sites of Tell Mozan (8444 fragments from 162 samples) and Tell Jerablus (8499 fragments from 80 samples). While a proportion of the samples derives from flotation contexts, many also represent hand-picked samples. The charcoal identification results are calculated as find percentages. The indeterminate category, that consisted of fragments that could not be identified into detail due to e.g., size or lack of literature, was excluded from the calculations. Sample by sample results with contextual information have been published previously in Deckers 2010, and Wilkinson and Deckers 2015 and a summary of some Jerablus samples in Deckers and Riehl 2007. Almost all samples were retrieved from domestic contexts; only 4 were from grave fills. A summary of the sampled contexts is available in Table I.

	Jerablus			Mozan			
Context type	**IB**	**IIA**	**IIB**	**EJIII**	**EJIV**	**EJV**	**MBA**
hearth/oven		1	3				
ash around oven					1		
fill of pit		1	8		6	11	4
dump				31	13	1	5
fill of building		4					
fill		1	19	24	10	10	21
occupation deposit	1		7	4	5	1	1
floor			2				
storage jar/fill of pot		1	1				2
installation							1
pot spread			2				
brickfall					2		2
pisé fall							4
grave/grave fill			1				3
wall collapse			1				
slope wash			1				
wall			4				
indet.	1	5	16				
Number of samples	**2**	**13**	**65**	**59**	**37**	**23**	**43**
Number of fragments	**218**	**2929**	**5352**	**4182**	**2355**	**755**	**1152**

Table I. Contextual information for the charcoal samples from Tell Jerablus and Tell Mozan.

From those charcoal samples 328 oak fragments were selected based on the visibility of the rays, which may be obscured through charring or cracking, or due to small fragment size. The maximal diameter present was measured, respectively calculated in order to understand whether small, medium or large-size timber was used and from that to infer woodland management. Table II shows more detailed contextual information for the samples, as well as where subsamples from the same context were taken. While it cannot be excluded that samples from the same tree or branch may have been sampled especially when the same context was sub-sampled, overall, the large majority of the contexts that were investigated tend not to represent remains from a single firing event, but averaged out remains from multiple firing events, hence long-lasting fire-wood exploitation and in this way also are less likely to contain fragments from the same tree (Asouti and Kabukcu 2021). The investigated Mozan area does not show evidence for large-scale conflagration, but twenty-eight measured fragments from context Fs2083 (2300-2100 BC) derive from a building that shows evidence for burning and thus may contain charcoal not related with fuel use (cf. Table II). At Jerablus the IIA settlement was destroyed by a fire (Peltenburg 2016, Pfälzner 2010), however only very few fragments measured may relate to architecture and carpentry remains (cf. Table I and II).

All measurements for the diameter calculations were undertaken using a Keyence digital microscope. For the diameter measurements, trigonometry methods were generally applied (Paradis-Grenouillet et al. 2010), although in a few cases (3) whole transversal sections of a twig were available, meaning measurement could be performed with the circle tool. In 163 cases the isosceles triangle trigonometry method was applied, while in 162 cases, trigonometry based on a constructed right-angle triangle was used (Paradis-Grenouillet et al. 2010). Since according to Paradis-Grenouillet et al. (2013) the trigonometry method by use of an isosceles triangle appears to be the most accurate method, the trigonometry method with a right-angled triangle was only used when that method was not possible e.g., by the fragmentary state of the charcoal, that does not have the last annual ring preserved over the distance of two rays. The latter method was also applied to on an earlier batch of samples that are included into the statistics (Deckers 2016). Diameter assessment focused on larger fragments. Samples were selected based on the presence of minimally two well visible multiseriate rays over minimally 2 mm, mostly more though (see transversal fragment sizes in Table II). In order to understand the reproducibility of the measurements, they were repeated two or three times -in exceptional cases four times-. The measured values were averaged, and the standard deviation calculated (Table II). Four measurements were taken when one measurement was retrieved from another couple of rays that resulted in significantly different results. To avoid a sampling bias another measurement was done on this set of rays then. No bark or cambium could be detected in the samples.

Table II. Diameter measurements, standard deviations of the measurements, annual ring widths and growth rate calculations, fragment sizes and contextual information for samples from Tell Jerablus and Tell Mozan. Where possible fragment sizes are given based on transversal measurements along a ray and perpendicular on a ray.

Linear regression in combination with variance analysis was used to assess the correlation between the diameter and the standard deviation.

Additionally, from those fragments for which the diameter of the last preserved annual ring could be successfully measured, 1101 annual ring widths were measured. Previously measured annual ring widths as published in Deckers (2016) were also included in some of the analysis to add additional data. They derive from the same sites and periods (Table II).

The maximal diameters for the different sites and periods were compared with one another and with reference studies to investigate changes in woodland management and wood availability. A comparison with experiments on the charring of wood with a diameter of 15 cm provides information on the resulting distribution of fragments amongst the diameter classes (Dufraisse and García Martínez 2011). These results mirror the conceptual model that shows that the largest volume of charcoal material from a log lays within the largest diameter size class, it is the class near to the diameter of the log that is charred. On the contrary, the model also predicts that the smallest volume of wood in a charred trunk, will be represented by diameters within the lowest diameter class

(Dufraisse 2006). Additionally, our dataset was compared with diameter data from the site of Kaman-Kalehöyük in Turkey (Wright 2018). This is so far the only site that published diameter analysis results that can be compared with our data. It is, however, located ca. 500 km away. The samples from that site derive only from rubbish pits and hearth contexts (Wright 2018).

The annual ring measurements were used to calculate an average growth rate, and this was used to calculate an approximate cambial age for the last annual ring present, by assuming a constant growth (Table II). This calculation can only be an approximation since trees do not show constant growth, with variations a function of growing conditions (which forms the basis of dendrochronology) and life cycles (for example, young trees grow faster than older trees (Schweingruber 1993)).

The distribution of cambial age calculated through this method was then investigated. Combining cambial age and diameter data allows us to identify, for example, coppicing practices, since these should produce assemblages with large amounts of young small diameter twigs that typically lack fungal hyphae.

Finally, the distributions of the average ring width by period were analyzed. This could provide information on climatic changes through time. Water is critical for oak growth meaning reductions in soil moisture, and in the dry farming plains of Northern Mesopotamia therefore rainfall, will be especially visible in the width of the late wood (Griggs et al. 2007). The annual ring widths were also compared to ring width data from well published assemblages from the region, including Tille Höyük (Griggs et al., https://www.ncdc.noaa.gov/paleo-search/study/8516 accessed online 09.06.2020), Shiukh Fawqani and Horum Höyük (Pessin 2004), and to present-day data from Iran on oaks in various conditions (from dieback oak that were in poor condition by drought and human impact to healthy oak) (Tongo et al. 2020). To compare our charcoal values with present day growth we considered a shrinking of about 24% during former charcoalification as has been established through experimental charcoalification of oak (Paradis-Grenouilet and Dufraisse 2018).

Statistical tests were applied as suitable for the data available. Groups were always first checked for normality (Shapiro-Wilk test)**,** variance (Levene test) and number. Depending on these conditions, it was decided to either apply Welch with Games-Howell follow-up test and/or Kruskall-Wallis with Dunn´s test follow-up. All statistical tests were done at the significance level of $p<0,05$.

In order to investigate the impact of herbivore browsing on oak, 121 fragments of which the diameter was calculated, were previously investigated for signatures of browsing (Deckers 2016), that may consist of slow growth, abrupt growth reduction and improvement, irregular annual rings, unpronounced annual rings discontinuous vessel ring in early wood, lack of early wood vessels, small early wood vessels, collapse of wood structure, vessel collapse, lack of multiseriate rays, and disoriented woody structure. Not all these characteristics, however, can be exclusively assigned to browsing impact (Schweingruber 2001).

Furthermore, hollow ways have been mapped for the Upper Khabur Basin in Northeastern Syria based on CORONA satellite photographs to investigate possible land use zones (data from Ur 2010b). They are the imprints of ancient tracks, radiating from the archaeological sites, particularly well preserved in the Upper Khabur Basin, less in the Middle Euphrates region (Wilkinson 2004, 81-82, fig. 5.1). Though it is difficult to exactly date the ancient tracks, it is thought that most of them in this region date to the late fourth and 3rd millennium BC (Wilkinson et al. 2010; Ur 2009), contemporary with the charcoal samples. Hollow ways can be used as a proxy for delineating the area under agriculture. This approach assumes that flocks were prevented from trampling on cultivated land close to settlements but were allowed to roam freely in pastures. The creation of hollow ways is a result of the constrained movement between cultivated fields, and the fade out points of these features indicates the beginning of unconstrained movement, and therefore open pasture (Wilkinson

1994; Ur 2009). As such, the ends of the hollow ways radiating from a settlement provide evidence for the extent of cultivated land.

Besides the hollow ways potential vegetation for the 3rd and 2nd millennium BC was mapped based on GIS-modelling of the wild plant fruit/seed data from archaeological sites in that period and region to compare the charcoal results with. The methodology for this has been described in detail in de Gruchy et al. (2016) and is based on the principle that there are natural constraints, such as soil properties, elevation and slope that pose limits to where taxa can grow, while the associated habitats (fields, steppe, desert, maquis, meadows, etc.) serve to inform the type of land cover in the locations the taxa grow. While each individual taxon may grow in many different habitats, collectively the dozen or more taxa able to grow in a single space will share some common habitats more than others. In this way, the most common natural habitat between the taxa of a space has been interpreted as the potential land cover type of that space. Where two or more natural habitats were equally likely in a space, an 'all-of-the-above' approach is taken. For example, if desert and steppe were equally likely habitats in a space, that space is interpreted as desert steppe (see de Gruchy et al. 2016, p. 254). While in instances where steppe is the most common habitat, additional steps were taken to discern if the plants indicate a more grassy steppe or shrubby steppe (de Gruchy et al. 2016, p. 255). It should be noted that much of the land cover mapping in this area was based on the available soil map with a resolution of 1:500,000. This coarse resolution does not allow for the routine identification of more localized habitats, meaning zones such as riverine gallery forest have not been mapped.

Results

The anthracological results from Tell Jerablus show high percentages of *Populus* sp./*Salix* sp. and *Tamarix* sp (Fig. 2a). The proportions of *Populus* sp./*Salix* sp. to *Tamarix* sp. fluctuate somewhat by period, and from period IB (3500-3000 BC) and IIA (3000-2800 BC) only a few samples were investigated and thus the observed changes may be not representative. Besides the major two taxa, some other riverine taxa were present (Fig. 2b): *Fraxinus* sp. (ca. 15% in IB (3500-3000 BC), 1% in IIA (3000-2800 BC), 10% in IIB (2800-2250 BC)), *Ulmus* sp. (ca. 6% in IB (3000-2800 BC), *Platanus/Fagus* sp. (0,5% in IB (3500-3000 BC) and 0,6% in IIB (2800-2250 BC)) and *Clematis* sp. (0,02% in IIB (2800-2250 BC) (Fig 2b). Cultivated taxa, such as *Ficus* sp., *Vitis* sp., *Olea* sp. and *Phoenix* sp. were almost exclusively present in period IIB (2800-2250 BC) (ca. 2%), except for a small percentage of *Ficus* sp. from IIA (3000-2800 BC) (Fig. 2b). Imported taxa, like *Pinus nigra/sylvestris* and *Cedrus* sp. were present in periods IIA (3000-2800 BC) and IIB (2800-2250 BC), with proportionally more in IIB (ca. 8%) (Fig. 2b). Open oak woodland taxa were also present amongst the different periods, with deciduous *Quercus* sp. present in all the periods, with the highest percentages (ca. 4%) in period IIB (2800-2250 BC) (Fig. 2b). *Pistacia* sp. were present in layers from period IIB (2800-2250 BC) (0,4%) and IA (3500-3000 BC) (4%), while other taxa of open oak woodland such as *Juniperus* sp. (0,07%) and *Amygdalus* sp. (0,5%) were found only in period IIB (Fig. 2b).

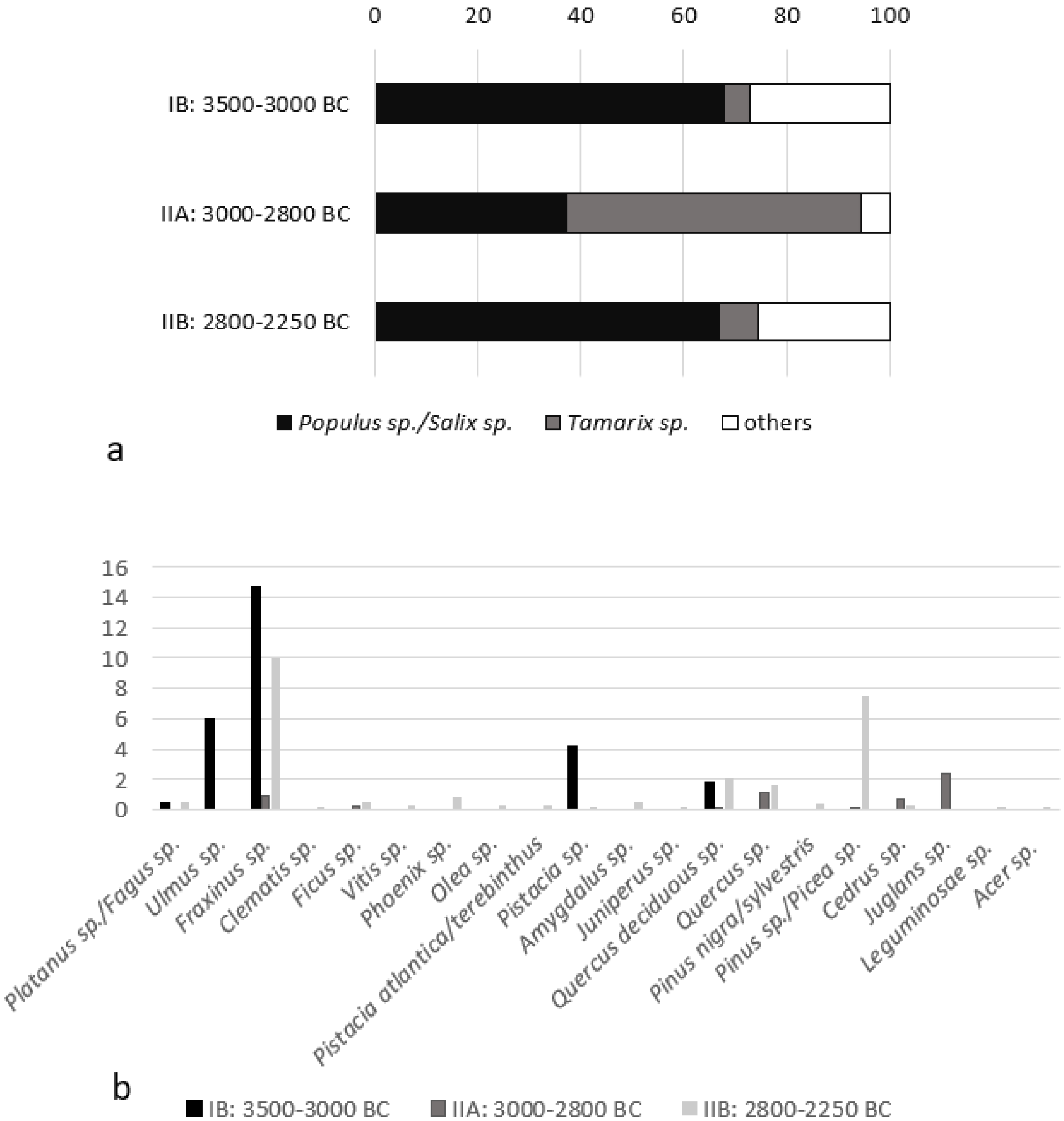

Fig. 2. Charcoal fragment count percentages from Tell Jerablus. a) Proportions of the most abundant taxa, b) Proportions of less common taxa ("others" in 2a). For details on the number of fragments and samples, see Table I.

The anthracological analysis from Tell Mozan indicates that oak – mostly, if not all, deciduous oak – was the proportionally most represented taxon amongst the charcoals, representing between 28% (MBA layers – 2000-1500 BC) and 92% (EJV – 2600-2300 BC) of the fragments identified across the different periods (Fig. 3). While *Quercus* sp. has its lowest percentages in the MBA layers (Fig. 3a), cultivated taxa, especially *Olea europaea* (ca. 41%) (Fig. 3a), but also *Vitis vinifera* and *Ficus carica* (Fig. 3b) increased compared to the previous periods. This increase coincides with proportionally more species associated with higher levels of moisture -possibly from riparian locations- in total percentages, including *Populus* sp./*Salix* sp. (ca. 11%), *Platanus* sp., *Ulmus* sp., *Fraxinus* sp. (Fig. 3b).

Additionally, compared to the Early Bronze Age there is an increased proportion of non-local taxa in MBA layers, especially of conifers like *Pinus brutia*/*halepensis* that have a circum-Mediterranean distribution (Zohary 1973: figs. 134 and 135) (Fig. 3b). However, although the proportion is high all remains were recovered from a single sample, a fill outside a house that appears to have belonged to elite (Pfälzner 2012).

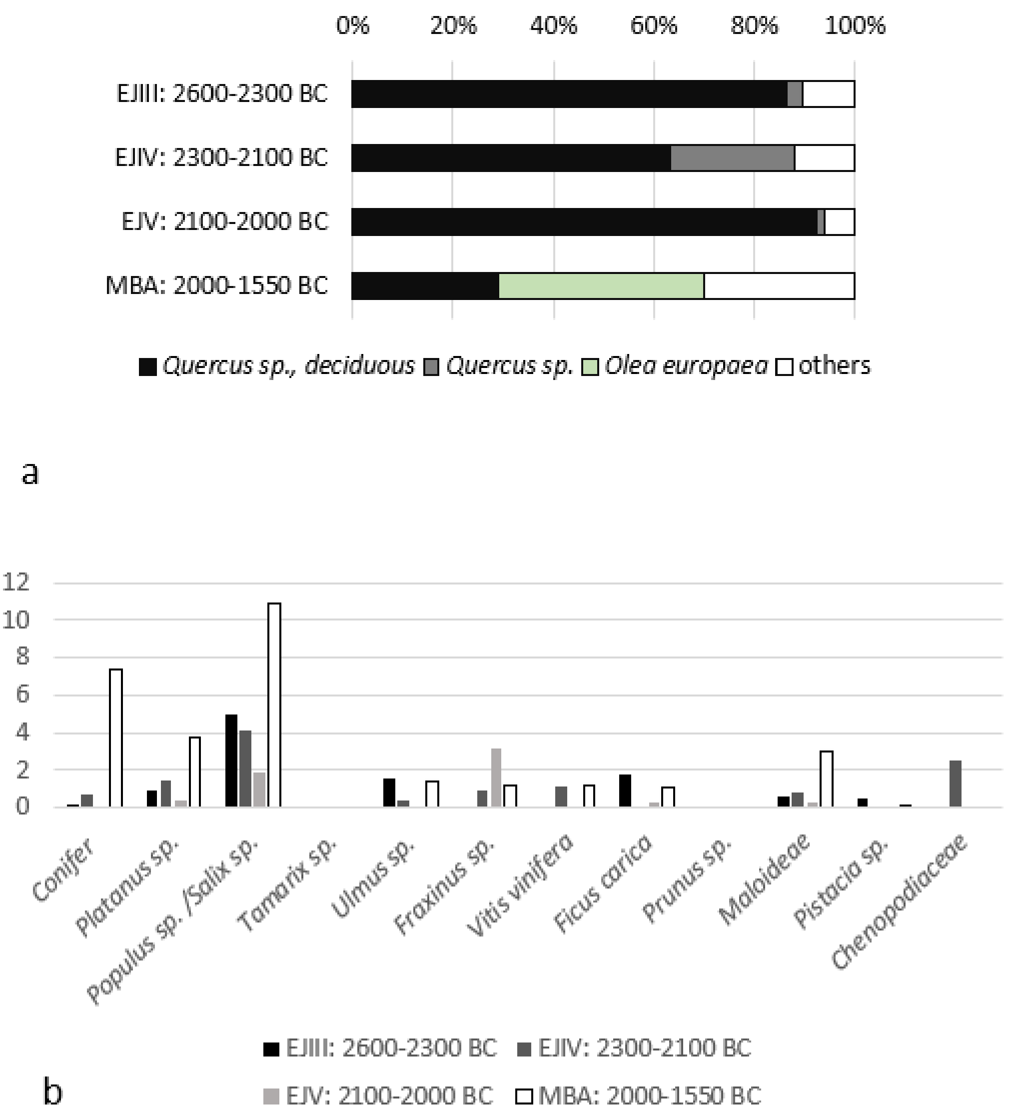

Fig. 3. Charcoal fragment count percentages from Tell Mozan. a) Proportions of the most represented taxa, b) Proportions of less common taxa. For details on the number of samples and fragments see Table I.

Regarding the deciduous *Quercus* sp. diameter measurements, linear regression analysis in combination with variance analysis shows a very high significant correlation between diameter measurements and standard deviation (p value 0,001); more precisely, the larger the diameter, the larger the standard deviation for the different measurements is (Fig. 4). Previous research found that diameter measurements of more than 20 cm are unreliable (Paradis-Grenouillet et al. 2013).

Therefore, we put all the large diameter measurements in Fig. 6 in one diameter class “more than 15 cm”, indicating large diameters which cannot be measured precisely.

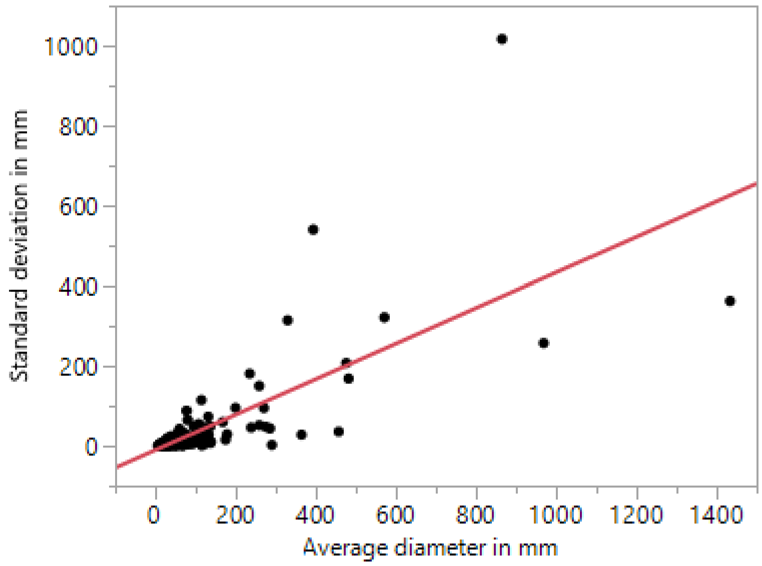

Fig. 4. Linear regression of standard deviation over the average diameter for the diameter measurements on oak.

The boxplot diagrams for oak diameter summarized according to the age of the sample context show that approximately half of the values are below 5 cm in all periods and that 75% of samples have a diameter clearly below 10 cm in all periods (Fig. 5). Based on non-homogeneous variance, non-normal distribution and low sample number for some groups, a Kruskall-Wallis test on the dataset was performed that shows no significant differences at the level p<0,05 in the distribution of the samples (Chi square = 5,41, p = 0,372, df = 5).

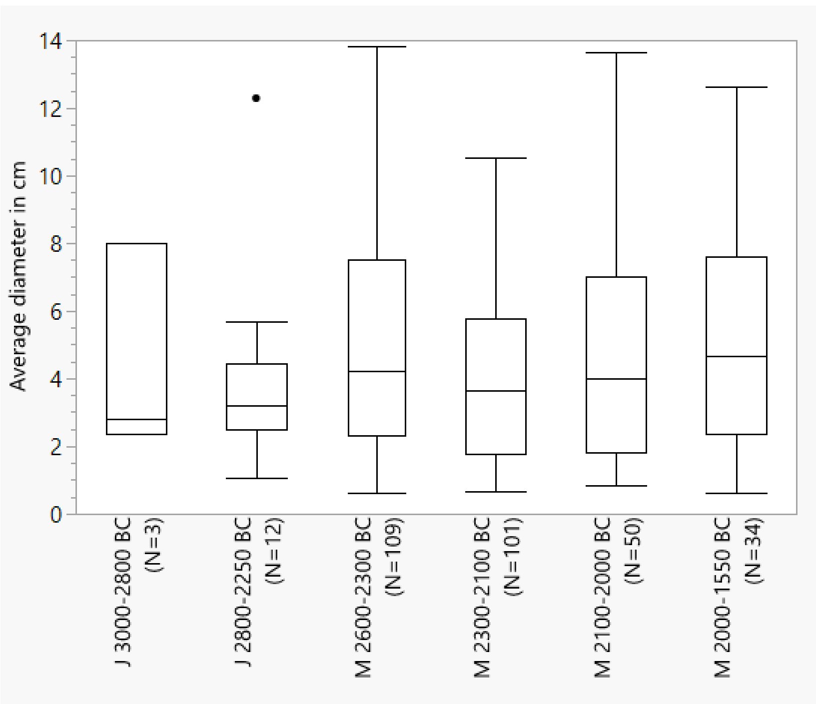

Fig. 5. Boxplot diagrams of oak diameters according to the period (i.e., the age for the layers the charcoal was found in). Samples that could not be assigned that precisely to one of the periods detailed were omitted.

In figure 6 the diameter data of oak for the different phases is summarized in diameter classes and compared with the diameter distribution for published reference data of a 15 cm diameter log (Dufraisse and García Martínez 2011) and data from Kaman-Kalehöyük in Turkey (Wright 2018). The two northern Syria sites show a different pattern to both Kaman-Kalehöyük and the 15cm log burning, with a greater proportion of the assemblage in the 0-5cm range and a lower proportion of larger fragments.

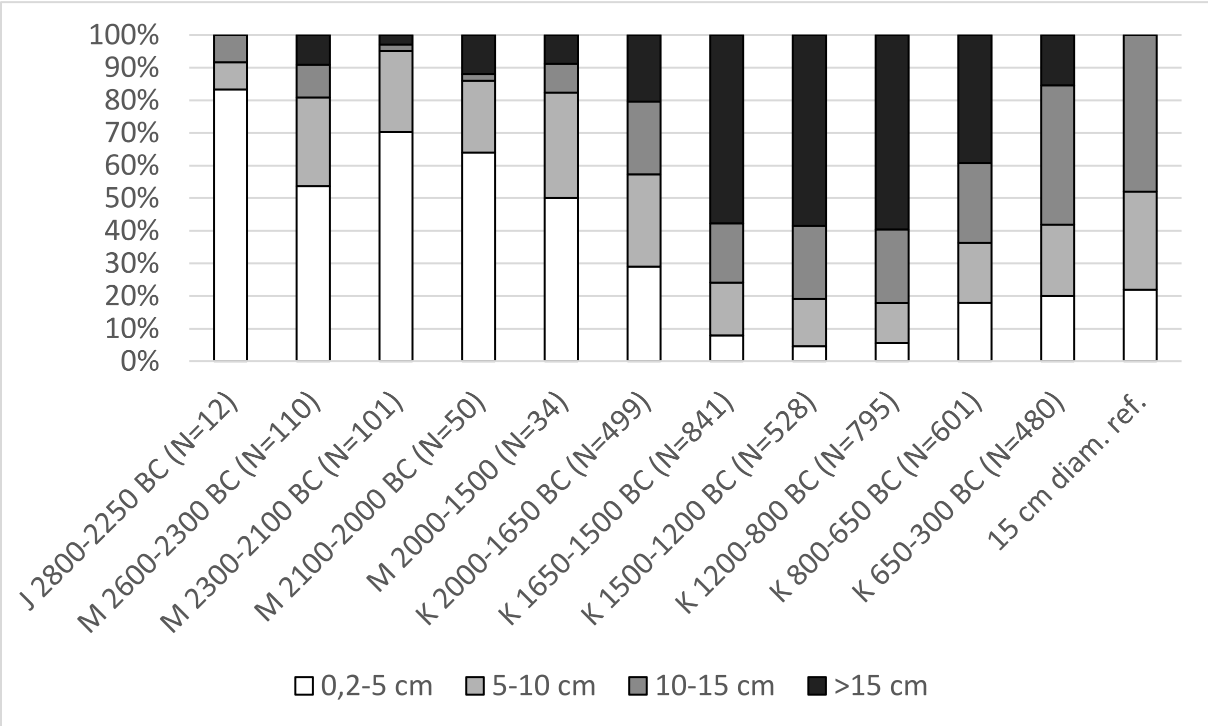

Fig. 6. Distribution of charcoal diameters amongst diameter classes for the different periods. The reference data, indicated with „ref.“, is for a 15 cm diameter log.J= Jerablus, M= Mozan, K= Kaman-Kalehöyük

The results of the cambial age estimation for the last available annual ring on the charcoal fragments show that just under half of the fragments represent cambial ages of 35 years or less (81 fragments), while just over half were older (85 fragments) (Fig. 7), including trees which seem to have been 730 and more than 900 years old. The 900-year-old tree has a diameter measurement of only 57 cm which would equal about 70 cm by calculating a 24% shrinking during carbonization, which can be considered as slow growth. The 730-year-old oak had a diameter of ca. 1 m, which would have been without shrinking during carbonization ca. 1,24 m, which is more substantial. Compared to these values, in temperate regions oaks of 730 or 900 years, would often be more than double this size (e.g., Haneca 2005). An estimated value of 2520 years old was omitted from the graph since it was likely an overestimate (Sample MZ01_q2866a_3). It should be noted though that also the 900- and 730-year estimates may be overestimates since the slow growth measurements were done on wood of old cambial age, which grows slower than wood from young cambial age (Schweingruber 1993). While we try to detect chronological trends in the data, the results shown in Fig. 7a and b indicate that we should keep in mind during interpretation that oak trees can be long-lived; and that the measured annual ring widths and diameters may not be directly dated to the context in which they were recovered.

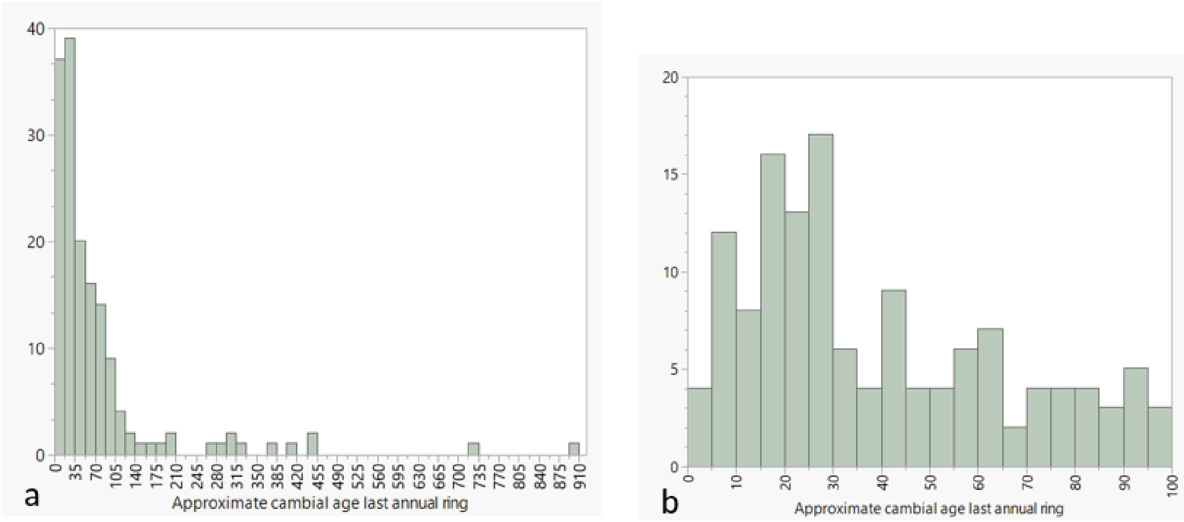

Fig. 7. a. Distribution of number of oak samples according to their approximate cambial age of the last preserved annual ring. b is a zoomed in version of a. Sample MZ01_q2866a_3 with an estimated cambial age of 2520 years is not depicted. b. Zoom-in of figure a within the reach of 0-100 years of approximate cambial age of last preserved annual ring.

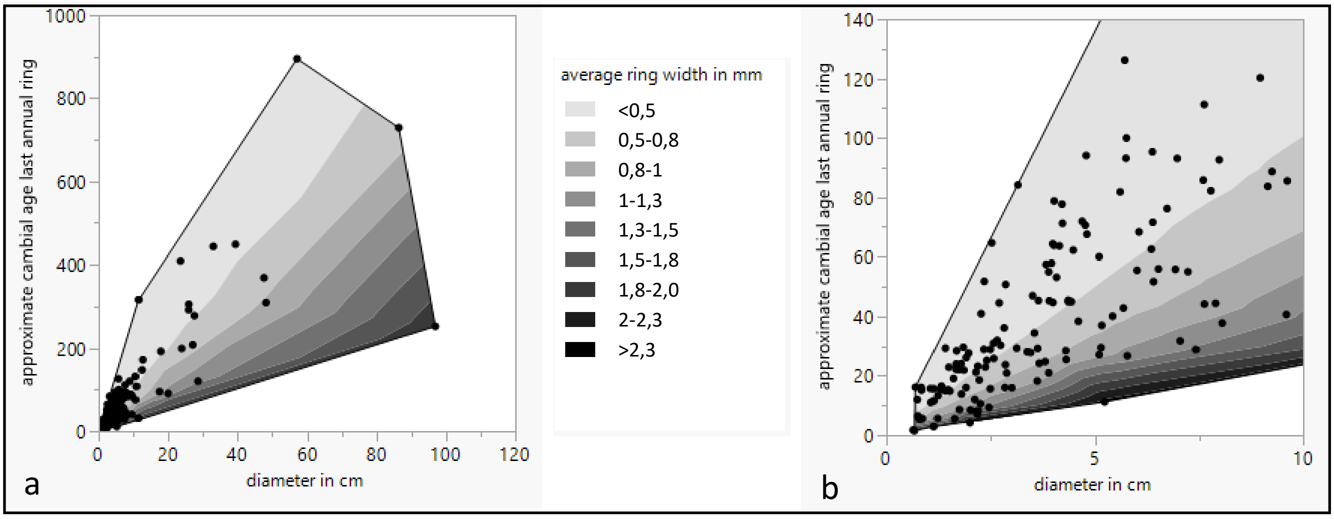

Fig. 8. Approximate cambial age of the last preserved annual ring versus diameter in cm of oak with indication of the average ring width – a. all the data from Tell Mozan and Jerablus, b. detail of the data.

Figure 8 plots the diameter, cambial age and growth rate. The lighter grey sections indicate slow growth, while the darker greys the opposite. Because the data are clustered in the light grey sections, we can infer slow growth is common. Only 16 fragments had a minimal estimated cambial age below 10 years, while only 3 were below 4 years.

Some differences over time are visible in the boxplots that depict the distribution of the measurements of the last preserved annual ring over time (Fig. 9). In particular, the median of the approximate cambial age of the last preserved annual ring from Middle Bronze Age Mozan (M 2000-1550 BC) appears to be higher than in previous periods. Half of the measured values were above 52 years old. In the previous periods at Mozan the median has changed from 37 years in the period between 2600-2300 BC, to 30 years in the period between 2300-2100 BC, 45 years between 2100-2000 BC. Since the sample number was small and the data for the different groups was not always normally distributed, a Kruskall-Wallis test on the whole dataset was also performed, but no significant differences were visible at the level p<0,05 in the distribution of the samples (Chi square = 6,70, p = 0,242, df = 5).

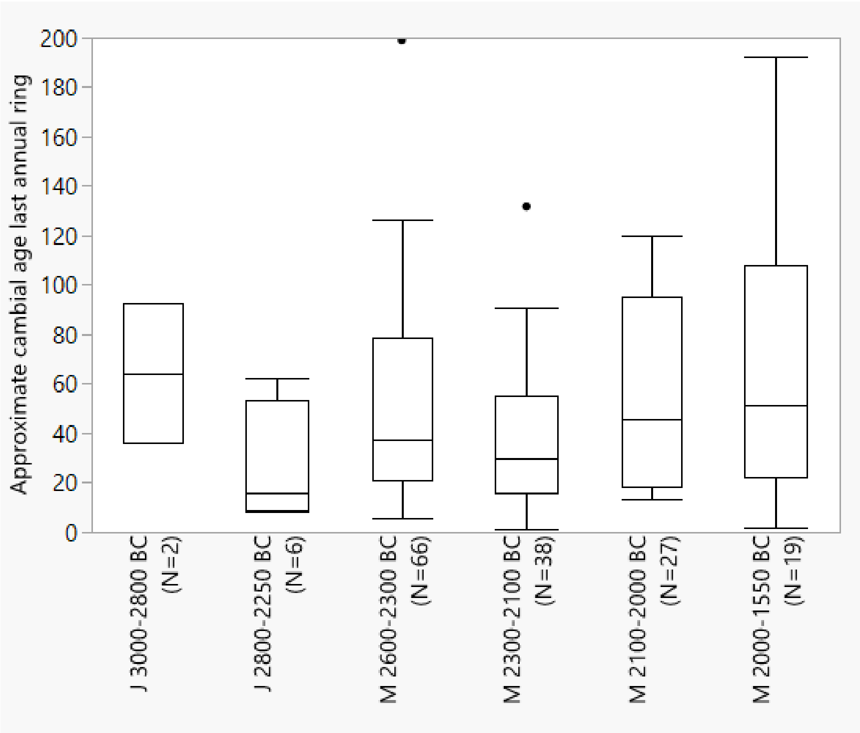

Fig. 9. Boxplot diagrams that show the distributions of the last preserved annual ring versus the period of the samples for oak (zoomed in into the reach of 0-200 - not all outliers are visible). Sample MZ01_q2866a_3 was omitted from the analysis as well as samples that did not belong to one of the periods detailed.

Figure 10 shows box-plot diagrams for the ring width of the samples for the different periods. Most marked is the boxplot with the ring widths for the period between 2100-2000 BC from Mozan. The median is smallest for this period, being 0,4 mm. Additionally, 75% of the measurements are smaller than 0,5 mm, whereas the 3rd percentile for the other periods is higher, between 0,8 and 0,7. Since unequal variances occur, the data is not normally distributed and not all groups have more than 30 samples, a Kruskall-Wallis test was undertaken on the whole dataset. However, no significant differences could be observed (Chi square = 8,40, p = 0,142, df = 5). On a smaller dataset with only those groups with 30 or more observations (see Fig. 10), a Welch test was performed, that showed significant differences for the means of Mozan 2600-2300 BC, Mozan 2300-2100 BC and Mozan 2100-2000 BC at a 0,05 significance ((F (2, 75,26) = 4,92, p= 001). A Games-Howell follow-up test showed that the significant difference was between 2600-2300 BC and 2100-2000 BC, while no significant difference could be discerned between 2600-2300 BC and 2300-2100 BC and between 2300-2100 and 2100-2000 BC.

The average ring width for charcoal samples from all periods from both sites is 0,58 mm. Considering the 24% shrinkage due to charcoalification, an average annual growth of 0,7 mm is calculated, with a range between 0,2 and 2,9mm.

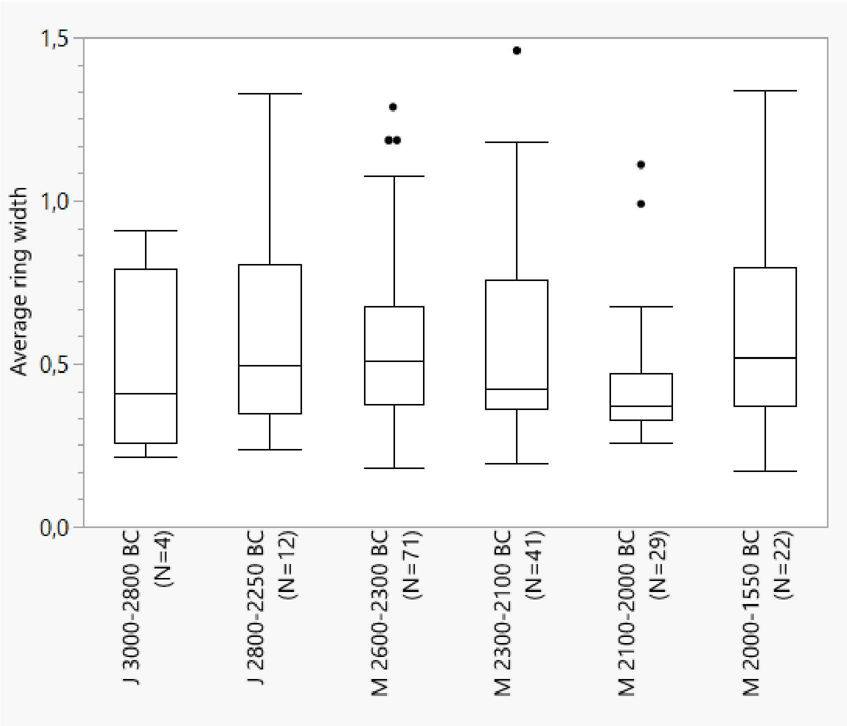

Fig. 10. Boxplot diagrams of oak fragments showing the distribution of the average ring widths/fragment for each period (some outliers are not visible due to zooming in). Samples that did not belong to one of the periods detailed are excluded.

An overview of the available comparison data on annual ring widths, all corrected for the 24% shrinkage, is visible in the boxplots of Fig. 11. Ring width data for oak charcoal was found for Tille Höyük located approximately 100 km north of Jerablus in Turkey, (Griggs et al. https://www.ncdc.noaa.gov/paleo-search/study/8516, accessed online 09.06.2020), Horum Höyük on the Middle Euphrates in Turkey somewhat north of Jerablus (Pessin 2004) and Tell Shiukh Fawqani on the Middle Euphrates in Syria, just to the south of Jerablus (Pessin 2004) (figure 1). Both Tille and Horum experience a slightly moister climate than Jerablus in the present day, while Shiukh Fawqani is close enough for the climate to be considered identical. Additionally, some present-day ring width values for oak in different health statuses were also available for *Quercus brantii* from the Ilam region in Iran today (Tongo et al. 2020). The latter region receives slightly more rainfall and has lower temperatures than our research area in the present day as it is at a higher elevation.

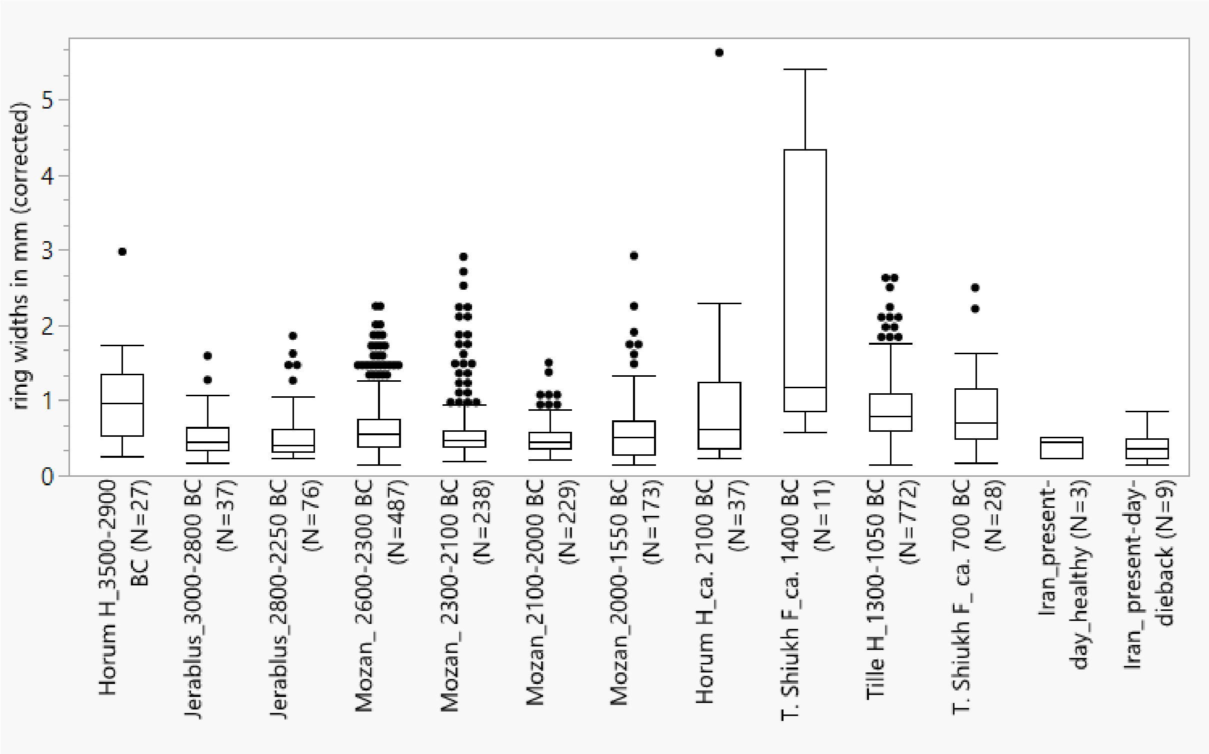

Fig. 11. Boxplots that show the distribution of the oak ring width data from Mozan and Jerablus compared with those from the archaeological sites Tille Höyük (Griggs et al. https://www.ncdc.noaa.gov/paleo-search/study/8516, accessed online 09.06.2020), Horum Höyük and Shiukh Fawqani (Pessin 2004). In order to be able to compare the charred archaeological data with the present-day values for Iran, a correction of 24% has been calculated. N refers to average ring width/fragment for Horum Höyük and Tell Shiukh Fawqani, to average ring width/region for Iran, whereas to individual ring width measurements for Mozan, Jerablus and Tille Höyük.

A Kruskall-Wallis test was performed since not all data has a normal distribution and the variance is unequal, as well as there are samples with few observations. The results indicate that not all distributions are the same (Chi square = 479,87, p = < 0,0001, df = 12). A follow-up Dunn´s test shows that the groups as depicted in Table III differ. Besides the in fig. 11 visibly differing Shiukh Fawqani_ca. 1400 BC and Mozan (all periods) and Fawqani_ca. 1400 BC and Jerablus (all periods), also significant differences in the distributions have been detected between Tille Höyük and Mozan (all periods), Tille Höyük and Jerablus (all periods), Shiukh Fawqani_700 BC and some periods from Mozan and Jerablus. Furthermore, also the distributions of the present-day Iranian dieback samples differ from those of Shiukh Fawqani_ca. 1400 BC, Horum Höyük_3500-2900 BC, and Tille Höyük. Moreover, there are also differences in the distributions of the Mozan 2100-2000 BC samples and those from 2600-2300 BC of the same site. Finally, the Horum Höyük_3500-2900 BC samples differ from the Mozan samples and 3000-2800 BC Jerablus samples.

Groups that show significant differences		p-value
Shiukh Fawqani_ ca. 1400 BC	Mozan_ 2600-2300 BC	0,00
Shiukh Fawqani_ ca. 1400 BC	Mozan_ 2300-2100 BC	<,0001
Shiukh Fawqani_ ca. 1400 BC	Mozan_ 2100-2000 BC	<,0001
Shiukh Fawqani_ ca. 1400 BC	Mozan_ 2000-1550 BC	<,0001
Shiukh Fawqani_ ca. 1400 BC	Jerablus_ 3000-2800 BC	<,0001

Shiukh Fawqani_ ca. 1400 BC	Jerablus_ 2800-2250 BC	<,0001
Tille Höyük_1300-1050 BC	Mozan_ 2600-2300 BC	<,0001
Tille Höyük_1300-1050 BC	Mozan_ 2300-2100 BC	<,0001
Tille Höyük_1300-1050 BC	Mozan_ 2100-2000 BC	<,0001
Tille Höyük_1300-1050 BC	Mozan_ 2000-1550 BC	<,0001
Tille Höyük_1300-1050 BC	Jerablus_ 3000-2800 BC	<,0001
Tille Höyük_1300-1050 BC	Jerablus_ 2800-2250 BC	<,0001
Shiukh Fawqani_ 700 BC	Mozan_ 2100-2000 BC	0,00
Shiukh Fawqani_ 700 BC	Mozan_ 2300-2100 BC	0,01
Shiukh Fawqani_ 700 BC	Mozan_ 2000-1550 BC	0,02
Shiukh Fawqani_ 700 BC	Jerablus_ 2800-2250 BC	0,00
Horum Höyük_ca. 2100 BC	Mozan_ 2100-2000 BC	0,01
Mozan_ 2100-2000 BC	Mozan_ 2600-2300 BC	<,0001
Mozan_ 2600-2300 BC	Horum Höyük_3500-2900 BC	0,00
Mozan_ 2000-1550 BC	Horum Höyük_3500-2900 BC	<,0001
Mozan_ 2300-2100 BC	Horum Höyük_3500-2900 BC	<,0001
Jerablus_ 3000-2800 BC	Horum Höyük_3500-2900 BC	0,00
Jerablus_ 2800-2250 BC	Horum Höyük_3500-2900 BC	<,0001
Mozan_ 2100-2000 BC	Horum Höyük_3500-2900 BC	<,0001
present day-dieback	Shiukh Fawqani_ 700 BC	0,04
present day-dieback	Tille Höyük_1300-1050 BC	0,00
present day-dieback	Horum Höyük_3500-2900 BC	0,00
present day-dieback	Shiukh Fawqani_ ca. 1400 BC	<,0001

Table III. Results of the Dunn´s test on the ring-width dataset. Only those groups that showed significant differences are depicted with their p-value.

A Welch test on a reduced dataset with only groups with more than 20 observations included (cf. Fig. 11), also suggests that not all means are the same (F (9, 213,77) = 54,44, p=<0,001). A follow-up Games Howell test indicates that Horum Höyük samples from 3500-2900 BC and the different Mozan phase samples are significantly different for their means. Also the Tille Höyük samples differ from Mozan and Jerablus samples from the different phases. Furthermore, the Mozan 2300-2100 BC and 2600-2300 BC samples differ significantly for their mean from the Mozan 2100-2000 BC samples (Table IV).

Site and period	Results of the GH test			Mean in mm
Horum Höyük_3500-2900 BC	A			1,03
Horum Höyük_ca. 2100 BC	A	B	C	0,92
Shiukh Fawqani_ ca. 700 BC	A	B		0,89
Tille Höyük_ 1300-1050 BC	A			0,88
Mozan_2600-2300 BC		B		0,63
Mozan_2300-2100 BC		B		0,59
Mozan_2000-1550 BC		B	C	0,57
Jerablus_2800-2250 BC		B	C	0,53
Jerablus_3000-2800 BC		B	C	0,53
Mozan_2100-2000 BC			C	0,49

Table IV. Mean corrected annual ring width for different sites and results of the Games Howell test on annual ring width for the different sites. Sites that are not connected by the same letters differ significantly. A correction factor of 24% shrinking has been applied.

Possible morphological signatures for the impact of browsing have been found on 12 of the 121 oak charcoal fragments from Mozan. These consisted of the lack of early wood vessels, irregular annual rings, disoriented structures, discontinuous thick rays, and vessel collapse (as previously published in Deckers 2016). No charcoals from other sites were investigated for these signatures so far.

In Figure 12 the potential vegetation based on the GIS modelling of archaeobotanical fruit/seed remains for the 3rd and 2nd millennium BC is depicted, as well as the hollow ways assumed to date mainly to the 3rd millennium BC. Hollow ways, that possibly delineate the area occupied by cultivation, indicate that a large part of the Upper Khabur Basin was used for agriculture. It is likely that further areas were under cultivation, but the hollow ways have not survived later processes of landscape transformation, such as heavy ploughing and later irrigation schemes. While dry shrub steppe appears to have been strongly represented in the 3rd millennium BC, in the 2nd millennium BC this vegetation type was clearly reduced.

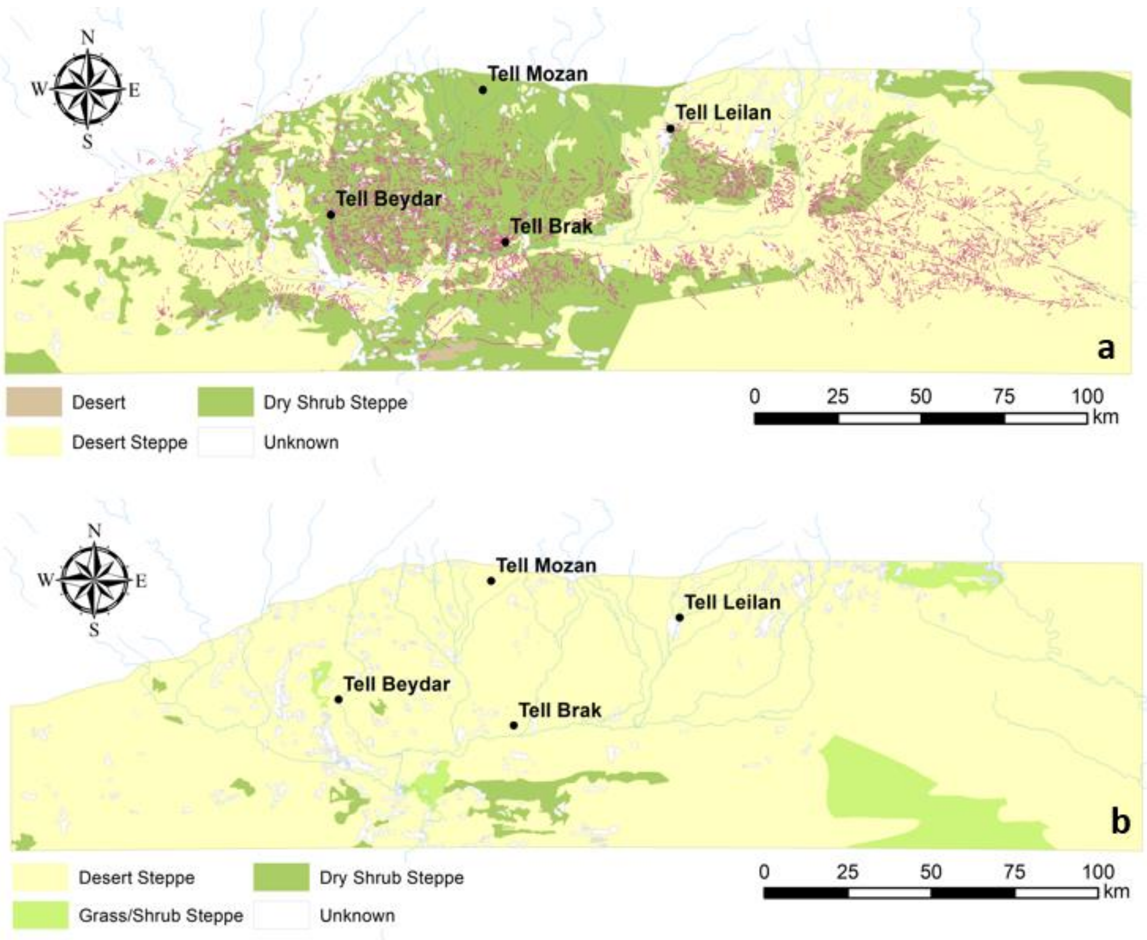

Fig. 12. Potential vegetation maps of the Upper Khabur Basin in north-eastern Syria for the 3rd millennium BC (a) and 2nd millennium BC (b) based on vegetation modelling in GIS using archaeobotanical wild plant seed/fruit remains. On map (a) also the hollow ways are indicated (pink linear features) (data from Ur 2010b).

Discussion

Former southwards distribution of oak

The charcoal taxa proportions from Tell Mozan and Tell Jerablus are different from one another. This relates largely to the different location of the sites: While Jerablus sits along the Euphrates River and is dominated by riverine taxa (such as mainly *Populus*/*Salix* and *Tamarix*), Tell Mozan was located on a much smaller and intermittent wadi in the Upper Khabur Basin, and as with other sites in the region (Deckers 2016) oak woodland taxa were most common. Oak is present at Jerablus, and other sites along the Middle Euphrates (Deckers 2019), but in small proportions, 4% in period IIB (2800-2250 BC), and no higher than 14% at other sites with a marked gradient from north to south likely a result of rainfall gradients. Based on the present-day vegetation, Hillman (in Moore et al. 2000) suggested that the potential vegetation of the Upper Khabur Basin and the Middle Euphrates at Jerablus discounting the Euphrates valley riparian forest, would have been deciduous oak-Rosaceae park woodland.

Unfortunately, it is not possible to identify oak charcoal to the species level. Although no oak is present in northeastern Syria today, based on the oak distribution maps from Zohary (1973) we deduce that *Quercus brantii* would be the most likely candidate (Fig. 13). Today, this tree species typically overlaps with steppe vegetation, as well as being associated with *Q. infectoria* ssp. *boisseiri*, Rosaceae species, and *Pistacia atlantica/terebinthus*. Further north, the number of associating trees increases and under more favourable conditions *Q. brantii* is even replaced by *Q. infectoria* ssp. *boissieri* or/and *Q. libani* (Zohary 1973).

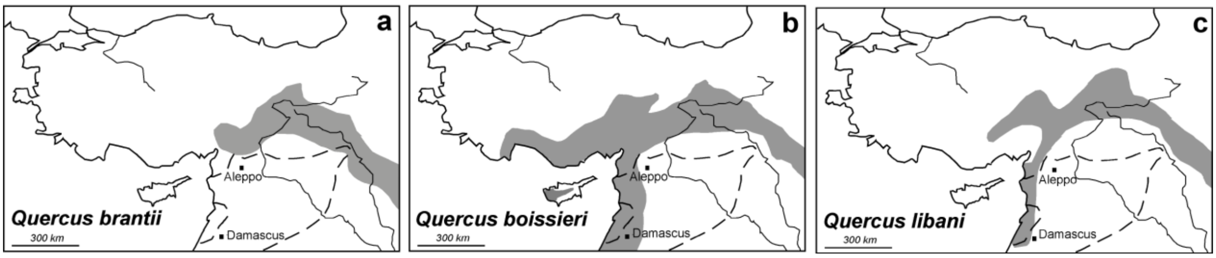

Fig. 13. Distribution of a) *Quercus brantii*, b) *Quercus infectoria boissieri* and c) *Quercus libani* (after Zohary 1973).

Evidence for oak management, coppicing or pollarding?

Q. brantii trees and oak in general are considered valuable resources in the Near East. They have been exploited for food (Mason and Nesbitt 2009), fodder, building material, fuel, shade, and leather tanning, and are often deliberately managed to enhance resource gain (e.g., Valipour et al. 2014; Soltani et al. 2015). In the northern Zagros of Iran, for example, silvopastoral management of oaks traditionally consists of “Galazani” treatment, which comprises the harvesting of pollarded trees on a 3 to 4-year cycle for animal fodder in winter. Additionally, this manipulation of the tree causes the presence of enough herbaceous cover for animal browsing in the dry season (Valipour et al. 2014). In the Tur´Abdin in Eastern Turkey, just north of the Syrian border and Tell Mozan, shredding (removal of the lower branches) and coppicing are practiced, while some trees are allowed to grow bigger for acorn production (Mason and Nesbitt 2009). In Central Anatolia there is widespread evidence for oak woodland management, consisting of coppicing, pollarding, and shredding, while large areas of oak woodland pasture have also been attested (Asouti and Kabukcu 2014). Most of these kinds of woodland management practices would typically result in the presence of small diameter charcoal fragments within the archaeological record, which is the case in Northern Syria, with between 30% and 83% of measured fragments having a diameter less than 5 cm and between 80 and 96% a diameter less than 10 cm.

However, the cambial age distribution of the last preserved annual ring indicates that the majority of wood present at the sites had an estimated cambial age of more than 35 years, which is approximately the longest known coppicing interval (Nicolescu et al. 2017). As mentioned above, oak harvesting cycles in adjacent areas are only about 4 years. Therefore, the presence of many small diameters amongst our data may be the result of slow growth. An average growth rate of 0,7 mm/year implies a radial growth of about 14 cm in 100 years, while the minimal growth that was measured of only 0,20 mm would imply a trunk with a diameter of only 4 cm in 100 years. This fits well with vegetation reconstructions based on wild plant seeds from archaeological sites that indicate a dry shrub steppe -almost as dry as a desert but with small trees or shrubs (de Gruchy et al. 2016, 254)- occurred across the Khabur Basin Plains of Northeastern Syria in the Early Bronze Age, up to about the limit of present-day dry farming (de Gruchy et al. 2016; ADEMNES) (Fig. 12). Moreover, there are indications that dung was used as an additional fuel in Tell Mozan, which may suggest -if dung was not the preferred fuel (Peña et al. 2003)- that wood resources were not that plentiful available (Deckers 2016), since the woody vegetation was rather open and mostly shrub was available.

A Kruskall-Wallis test could not detect significant differences in the distributions between the samples from dieback oak in Iran and the samples from Mozan or Jerablus, while the Tille Höyük samples for example were significantly different for their distribution (Table III). The dieback of oak in Iran today is due to climatic drying, overgrazing, understory cropping and land-use changes that made the oaks prone to diseases (Tongo et al. 2020). Narrowest ring widths were observed in trees that showed strong dieback, but the average ring width values differed from area to area in Iran (Tongo et al. 2020). The largest average growth with strong dieback was 0,37mm per year and came from the Dalab woodlands. About 13% of the measurements from Tell Mozan and Tell Jerablus had a smaller annual growth than this figure, while 31% had annual growth values less than 0,47 mm. The latter value is the mean value for moderate dieback in Ilam (cf. Table III). Hence, a proportion of the oak in Mozan and Jerablus seems to have grown as slow as severe and moderate dieback oak from Iran, so it is possible that (some of the) oak was under pressure, perhaps through overgrazing.

Slow growth of oak and herbivore browsing

In the Karadag area in Turkey, slow growth in oak scrub is associated with intensive grazing by caprine herds and feral horses (Asouti and Kabukcu 2014). The morphological analysis of oak charcoals indicates that some may show morphological features of browsing. Studies on foraging behaviour of cattle and goats in oak woodlands in Greece have shown that while cattle only feed on herbaceous species, goats browse quite strongly on oak (41% of their total intake) and have a negative impact on the growth of the shoots (Papachristou and Platis 2011). Slow growth has often been cited in relation to herbivore browsing pressure, and the impact appears to increase closer to the limits of the natural habitat zone of the tree species (e.g., Speed et al. 2011; Trotter et al. 2002). Phytolith investigations of coprolites from Early Bronze Age Tell Abd, south of Jerablus along the Euphrates, demonstrates that sheep/goat were grazing in woody areas or fed by additional woody fodder (Riehl 2019). Besides herbivores, omnivores can impact on oak woodland, e.g., pigs by rooting. This causes a decrease in aboveground biomass and reduces the survival of tree seedlings, limiting tree regeneration and reproduction (Sweitzer and Van Vuren 2002). Enamel investigations on pig teeth from the study region (Leilan) indicate changes over time in the management of pigs, with more indications of stress after 2600 BC, possibly related with increased penning of pigs and intensification (Price et al. 2017). Textual evidence also indicates that they were kept in pens rather than being herded by the 2nd millennium BC (Price et al. 2017). If these management practices were universal, pigs may have had some impact on woodland before 2600 BC but would not be responsible for the slow-growing oak after 2600 BC. The shift from free roaming to penning pigs may even have been a consequence of the depletion of oak woodland and the resulting absence of suitable foodstuffs such as acorns (Price et al. 2017), although more data is required to assess the validity of this argument.

Archaeozoological remains from sites in northern Syria indicate that during the fourth and 3rd millennium BC specialised pastoralism had developed (Zeder 1995). Evidence from Tell Mozan indicates that sheep and goat bones dominate the archaeozoological record, as was the case at most sites in the region, whereas pigs, accounting for up to 10% of the domesticated species, seem to have played a smaller role, but still important at the household level (compare Doll 2010 with Zeder 1995 and a summary in Price 2017). Estimations for land use in the 3rd millennium BC based on site sizes, population levels and pre-modern energy requirements have been calculated for the Upper Khabur Basin and suggest that the area was so intensively inhabited that hardly enough land was available for pasture, which implies impact on the oak woodland was likely if all the pasture took place in the surroundings of the sites (Deckers 2016, but also Wilkinson 1994, 2003 and Kalayci 2016). Based on the extension of hollow ways (cf. Fig. 12a) several scholars have inferred that the area available for pasture was extremely limited (Wilkinson 2003, Ur 2009). In these areas animals may have been taken further away from the site into the steppe beyond the cultivation zone and/or had to be fed by additional cultivated fodder, putting them into competition with people for food (Wilkinson 2003). More complex linkages between pastoralism and cultivation, such as the grazing of flocks on failed crops in bad years, may have been used to mitigate risk in areas where limited rainfall meant stable crop yields could not be guaranteed (see Wilkinson et al. 2014). In the Jerablus surroundings settlement density was lower than in the Upper Khabur region, but was still higher than in areas further south, and agricultural needs may have limited available pastoral areas (Wilkinson et al. 2012). Further work on local land use practices is required to fully contextualise our results.

Textual evidence indicates that pastoral activities during the Early Bronze Age were a major aspect of the political economy, with even higher numbers of animals than calculated in the estimations of Deckers (2016). At the Early Bronze Age centre of Tell Beydar, about 60 km southwest of Tell Mozan, ancient texts indicate that the central institution administered 7,400 sheep and goat (Sallaberger 2004). Texts from Ebla, located ca. 150 km southwest of Jerablus and likely the political centre of the entire region, indicate that urban institutions controlled large herds. The number of sheep under the control of the Ebla palace has been estimated as between 80 000 and 110 000 according to Archi (1993). He noted that these were only the sheep directly controlled by the palace, and we can assume that most rural communities had their own flocks. According to an estimate by Milano (1995), also based on the texts from Ebla, a flock would have consisted of 67 000 sheep and there would have been 10 of them, a total of 670 000 sheep. Regardless of the precise numbers, sheep rearing was a major economic activity and wool production was an important asset (e.g., Milano 1995; Doll 2010). However, in the calculations of the land needed to feed the people as undertaken in Deckers (2016), Wilkinson (1994) and others (e.g., Kalayci 2016), sheep for wool were not included. Despite this, all three reconstructions suggest there was hardly enough land available to feed the inferred human populations.

Extensive agricultural fields and their impact on oak woodland

The extensification of farming practices over the Late Chalcolithic and Bronze Age may also have put pressure on woodland resources (Styring et al. 2017), either by pushing pastoral activity into new areas or more directly by extending into wooded environments. The latter could include woodland clearance and replacement with cultivated fields, or by understory cropping. In particular, as in Iran, understory cropping may have caused reduced annual growth of the oaks (Tongo et al. 2020). While compared to animal husbandry, agriculture proportionally takes up less land per caloric output, the extension of hollow ways that delineate the agricultural land under use (Ur 2009; Ur 2010b) (Fig. 12a) and the calculations of agricultural land based on settlement size (Deckers and Riehl 2008; Deckers 2016), both indicate that a large area of the land was used for agriculture (see also Riehl 2010 and Kabukcu 2012), which may have been cleared of its woody vegetation. The charcoal data from Jerablus indicates that fruit tree cultivation may have been most intense in phase IIB (2800-2250 BC) (ca. 2%). No decrease in oak percentages is visible at that time, but this may also reflect the fact that only few charcoal samples have been investigated from the previous periods (see Table I). Additionally, due to the location of Jerablus at the Euphrates edge, it is likely that fields, vineyards and fruit orchards may have been located near to the Euphrates and thus mostly impacted the riverine woody vegetation and not the oak woodland. A reduction in riverine taxa from phase IA to IIB is visible and may be indicative of degradation of the riverine woodland diversity. Oak woodland may therefore have remained less affected by agriculture in that area.

In Mozan, on the other hand, cultivated charcoal taxa percentages were similarly high in the EJIII phase (2600-2300 BC) and slightly lower in the following Early Bronze Age phases (1% in the phase 2300-2100 BC, 0,2% in the phase 2100-2000 BC). Oak dominates this site and only diminishes during the Middle Bronze Age, when there was a peak in fruit tree taxa in the charcoal remains, up to 43% of the fragments identified (mostly olive). This shift to fruit tree exploitation occurred as the settlement diminished in size. Interestingly, no olive stones have been found in the Middle Bronze Age occupation layers (Riehl 2010), but this may be due to olive processing taking place at another location. Olive charcoal, possibly pruning waste, appears to have been more readily available from the Middle Bronze Age onwards at Mozan (Riehl 2010).

The impact of the fluctuating climate on oak and its growth

Besides human impact through pastoral activities and agriculture, climatic stress may also have been responsible for the slow growth of the oaks in northern Syria and a general reduction of oak woodland. The period under consideration here, between 3500 and 1550 BC, witnessed climatic fluctuations as reflected in a variety of local palaeoclimate records (Finné et al. 2019; Jones et al. 2019; Palmisano et al. 2021). The period between 3500 and 3000 BC appears to have been somewhat moister than today, with the first half of the 3rd millennium BC even wetter. From the second half of the 3rd millennium BC onwards climatic conditions became increasingly drier, with an arid peak around 2200 BC that was also seen in many other regions (e.g., summary in Kaniewski et al. 2018).

Although there is no pollen data for this region, anthracology has established that oak appears to have expanded to its maximum extent in the Fertile Crescent by the mid-Holocene. This also fits with the pollen data available to the north of our study region, that shows the maximal oak pollen expansion between 4000 and 2000 BC (Wick et al. 2003). Ideally, we could use the modern Iranian data to identify expected annual ring widths under different climatic conditions. It is of note that the sites that are located in moister conditions (like Tille Höyük and Horum Höyük) are significantly different from the Iranian samples in their distributions, whereas those from Mozan and Jerablus do not show significant differences. Interestingly, there are also significant differences in the means of the annual ring width between 2600-2300 BC and 2100-200 BC and 2300-2100 BC and 2100-2000 BC, with the smallest mean annual ring width for 2100-2000 BC, which is possibly related with the 2200 BC arid event. It is of note that at Mozan the upper quartile and upper whisker is lower than in other periods for the period 2100-2000 BC (Fig. 10), which may relate to aridity, causing fewer oaks with good growth. Further investigation is required to assess whether this aridity pattern for the phase 2100-2000 BC recurs when more measurement data becomes available, especially when data from the Middle Bronze Age can be added to the statistics. The pattern, however, may also have been caused by the fact that the measured annual rings of the charcoals may not be approximately related to the layer they were found in. The variety of the annual ring widths may also have been caused by possible different specific locations in the landscape.

Woodland Exploitation and Land Use during the Late Chalcolithic and Bronze Age

Our anthracological analyses demonstrate that there are clear differences in the types of woodland exploited at Jerablus and Mozan. Whereas the inhabitants of Jerablus were more reliant on riverine species, at Early Bronze Age Mozan people were more reliant on oak. This difference can be explained by the different locations of both sites, with Jerablus sitting right along the Euphrates, while Mozan is not located along a perennial river. The Euphrates woodland vegetation was not only lusher than the oak woodland further away from the river, it was possibly also the zone that was exploited most for agriculture. The find of burned dung pellets (Kabukcu 2012) in combination with riverine woodland at Jerablus even more so indicates that there was not much non-riparian woodland nearby.

Some shifts in the exploitation of woodland can be observed at both sites, most likely through the displacement of woodland by fruit tree cultivation, e.g., in phase IIB (2800-2250 BC) at Jerablus and from the MBA (2000-1550 BC) at Mozan. In Jerablus a smaller variety of riverine taxa were exploited from phase IIB (2800-2250 BC) onwards, when more fruit tree wood was used, likely the result of pruning. A similar change is visible from the MBA (2000-1550 BC) onwards in Mozan, when olive became the dominant taxon among the wood charcoal, possibly related to its local cultivation and the availability of pruning remains. Strangely this shift to olive exploitation is not reflected in the seed remains from the site, perhaps indicating specialized production either in part of the site which has not yet been excavated or in the local area, alternatively may indicate the wood was selected for a specific use. The increased abundance of grape pips in the later part of the MBA at Mozan may support an argument of a generally increased cultivation of fruit trees. The attendant reduction in use of oak at the same time as the increase in the proportions of olive wood in the record may also be indicative of a decrease in oak in the landscape, although this is difficult to disentangle using proportional data.

While oak has been exploited mostly for wood fuel and possibly also some carpentry (typically more after re-use as fuel) to a much lesser degree at Tell Jerablus than at Tell Mozan, its remains tell a similar story of exploitation. No systematic oak woodland management practices, such as coppicing or pollarding took place, indicating rather opportunistic wood use without much planning and effort, where necessary accompanied by dung as fuel. In Mozan for example, charcoal as well as a coprolite was found in an oven context, which suggests that the oak wood resources were scarce there (Deckers 2011), but also in Jerablus burned dung pellets were found throughout the site that indicate the use of dung as additional fuel (Kabukcu 2012) Often small diameter oak wood was used, that derived from shrub-like oak, that was growing very slowly. The slow growth was likely caused by intensive animal husbandry in this zone under arid conditions and perhaps also by understory cropping.

The additional use of dung as fuel probably caused a reduction in the availability of dung for manuring. As seen in Styring et al. (2017) fresh dung no longer seems to have been used as manure as indicated by the lower $\delta^{15}N$ values of crop remains from the Early Bronze Age compared to previously. However, Wilkinson (1989; 1994) has indicated that field scatters with pottery sherds indicate a zone of manuring surrounding many Early Bronze Age settlements. This manuring, however, would not have consisted of dung, but of ash from dung after it was used as fuel in the settlement and enriched with other household refuse, including the pottery sherds which make this practice visible archaeologically. The use of ash however, may have reduced the visibility of manuring in the $\delta^{15}N$ values of the crops since the charring of plant residues (as well as dung) at high temperatures causes a strong loss of N with little opportunity for fractionation (Saito et al. 2007). Lower N availability in the soils is also known to cause lower $\delta^{15}N$ values in the plants (Craine et al. 2015). Although the lower N levels suggest that the use of ash would be less effective than fresh manure, this kind of manuring is still valuable and practiced today in some areas (Wilkinson 1989). Given the decline in efficacy of ash over fresh manure, we might assume that past farmers would prefer to burn wood and manure fresh. The shift to ash may therefore be interpreted as enforced and related to an overall decrease in available woody resources (Shahack-Gross and Finkelstein 2008; Watson 1979). While dung was already used as fuel in Chalcolithic period sites (Miller and Marston 2012; Smith et al. 2019), it´s scale of use may have increased in the Early Bronze Age.

The trend in the use of wood from shrub-like oak appears to be consistent through time at both sites. Although the data from Jerablus is preliminary, a proportion of the oak seems to have grown slowly in the Late Chalcolithic. This implies that the land in the surroundings of Jerablus and Mozan was already heavily exploited by the Late Chalcolithic. Resource exploitation calculations, population calculations and inferred cultivation areas from hollow ways in the larger region have all suggested that the land was used at its limits in the Early Bronze Age (Deckers and Riehl 2008; Ur 2009; Deckers 2016; Lawrence et al. 2021) and so much land was under agriculture that areas available for pasture were severely constrained, just as large-scale exploitation of sheep for textiles was becoming a major part of the economy (Milano 1995; Archi 1993; Sallaberger 2004). In the North Jazira Survey (to the east, adjacent to our research area) it has even been suggested that the abandonment of a large part of the previously densely settled survey area during the Ninevite V period (c. 3000–2500 BC) was a deliberate strategy to make space for pastoralism (Wilkinson and Tucker 1995). Pasture probably put pressure on the oak, caused overgrazing, and generally may have resulted in desertification, as has been seen in many dryland environments (Zerboni and Nicoll 2018), including in the present-day Levant (Köchy et al. 2008), but also in Late Chalcolithic and Early Bronze Age Jordan (Henry et al. 2016). Settlement and radiocarbon proxy studies in Lawrence et al. (2021) indicate that the population had grown beyond sustainability in the Early Bronze Age, which made communities vulnerable to desertification and crop failure, especially with the additional 4,2 kyr BP drying. It is possible that geomorphological instability brought about by desertification may even have contributed to the formation of hollow ways, although more research is required to assess this.

The decrease in oak in favour of olive may be symptomatic of the depletion of oak in the site's surroundings at that time. The use of dung as an additional fuel in the Early Bronze Age at Mozan (Deckers 2011), but also at other Early Bronze Age sites, indicates that there was already some scarcity of woody resources, but limited depletion, in this region. Vegetation reconstructions based on seed data have shown an increase in desert-steppe environments in the Upper Khabur Basin during the Middle Bronze Age compared to the Early Bronze Age (de Gruchy et al. 2016) (Fig. 12). Despite both the impact of early urban societies and climatic drying by the end of the period under consideration, vegetation appears to have been lusher than today, with oak still having a more southwards distribution than at present.

Conclusion

This study has demonstrated the value of combining diameter with ring width data for reconstructing the presence and types of ancient woodland management practices. Without the ring-width data, incorrect anthracological conclusions would have been drawn. The triangulation method appears to be the best method in measuring diameters as investigated by Paradis-Grenouillet et al. (2013), but it should be remembered that it produces larger errors for large diameter fragments.

The anthracological analysis shows that the vegetation was lusher than today, with riverine gallery forest along the Euphrates and oak scrub-woodland away from the Euphrates and within the Upper

Khabur Basin. Oak had reached it maximal expansion into northern Syria in the mid-Holocene. The landscape, however, was not pristine, and consisted of extensive, large-scale agriculture surrounding the densely spaced settlements. The limited uncultivated land was likely used for potentially enormous herds of sheep and goat, which formed an important part of the economy. Both understory cropping and sheep and goat grazing, perhaps in combination with arid conditions, caused extremely slow growth of the oak, and most trees must have had a scrub-like appearance already by the Chalcolithic period. People exploited these oaks for fuel and possibly carpentry, in large proportions at Mozan and to a lesser extent at Jerablus and did not apply systematic woodland management practices at any point during the study period. They did use dung as an additional fuel (e.g., Mozan), probably to cover scarcity in fuel resources, which may have contributed to the increased use of dung ash instead of fresh dung as manure. It is this shift which brings material culture from household refuse into the manure, and results in the spreads of battered sherds recorded in archaeological surveys. More broadly, we see here impacts on the vegetation which could be related to overexploitation and unsustainable practices, making the land vulnerable to desertification and increased the risk of systemic collapse (Lawrence et al. 2021).

From the Middle Bronze Age onwards in Mozan, oak resources appear to have become more depleted. Olive wood was used more, which probably relates to a generally increased fruit tree cultivation that produced more readily available woody resources through regular pruning requirements. The decrease in oak at that time fits with the observed increase in desert-steppe environments in the seed remains from archaeological sites in the region during the Middle Bronze Age, but not with the absence of fruits of olive. It is possible that specialized olive production was taking place at an as yet unrecovered location. It seems unlikely that olive wood was imported for fuel in the absence of other olive products.

The charcoal analysis indicates that settlements impacted the vegetation. It seems that small as well as large settlements had a similar impact on the (oak) vegetation. Additionally, anthropogenic footprints are already visible from the Late Chalcolithic and throughout the period investigated, so the landscape was already heavily used before the Early Bronze Age major urbanization phase.

Acknowledgements

This research has received funding from the European Research Council under the European Union's Horizon 2020 research and innovation programme, grant agreement No. 802424, award holder Dr. Dan Lawrence. Many thanks are due to Dr. Jane Gaastra for critically commenting on a former draft of this manuscript and to Dr. Anne Wissing for providing contextual information of Mozan samples.

List of references

ADEMNES: The GRF (German Research Foundation) and University of Tübingen funded Archaeobotanical Database of Eastern Mediterranean and Near Eastern Sites, last update 2015. www.ademnes.de

Algaze, G. (2008) Ancient Mesopotamia at the Dawn of Civilization: The Evolution of an Urban Landscape. The University of Chicago Press, Chicago and London.

Arbuckle, B., Hammer, E.L. (2019) The Rise of Pastoralism in the Ancient Near East. Journal of Archaeological Research 27, 391–449.

Archi, A. (1993) Trade and Administrative Practice: The Case of Ebla. Altorientalische Forschungen 20, 43–58.

Asouti, E., Kabukcu, C. (2014) Holocene semi-arid woodlands in the Irano-Anatolian region of Southwest Asia: natural or anthropogenic? Quaternary Science Reviews 90, 158-182.Buccellati, G., Kelly-Buccellati, M. (1999) Das archäologische Projekt Tall Mozan/Urkeš, Mitteilungen der Deutschen Orient-Gesellschaft zu Berlin 131, 7-16.

Burke, A.A. (2014) Amorites, Climate Change, and the Negotiation of Identity at the End of the Third Millennium B.C. In: Höflmayer, F. (Ed.) The late third millennium in the ancient Near East chronology, C14, and climate change. Oriental Institute Seminars 11. Chicago, Illinois, 261-307.

Charles, M, Pessin, H, Hald, M. (2010) Tolerating change at Late Chalcolithic Tell Brak: responses of an early urban society to an uncertain climate. Environmental Archaeology 15.2, 183-198.

Craine, J.M., Brookshire, E.N.J., Cramer, M.D., Hasselquist, N.J., Koba, K., Marin-Spiotta, E., Wang, L. (2015) Ecological interpretations of nitrogen isotope ratios of terrestrial plants and soils. Plant soil 396, 1-26.

Deckers, K. (2010) Anthracological research at Tell Mozan. In: Deckers, K., Doll, M, Pfälzner, P., Riehl, S. (eds.) Development of the Environment, Subsistence and settlement of the city of Urkes and its region. Studien zur Urbanisierung Nordmesopotamiens, Serie A 3. Harrassowitz, Wiesbaden, pp.361-378.

Deckers, K. (2011) The dung as fuel model tested at two Syrian Jezirah sites. In: Deckers, K. (ed.) Holocene landscapes through time in the Fertile Crescent, 143-156.

Deckers, K. (2016) Oak charcoal from northeastern Syria as proxy for vegetation, land use and climate in the second half of the Holocene. Review of Palaeobotany and Palynology 230, 22-36.

Deckers, K. (2019) 13. Charcoal remains from 3rd millennium BC Tell el-Abd. In: Finkbeiner, U. (Ed.) Final Reports of the Syrian-German Excavations at Tell el-ʻAbd, Volume III. Zaphon Verlag, 187-190.

Deckers, K., Pessin, H. (2010) Vegetation development in relation to human occupation and climatic change in the Middle Euphrates and Upper Jazirah (Syria/Turkey) during the Bronze Age. Quaternary Research 74, 216-226.

Deckers, K., Pustovoytov, K. (2011) Geoarchaeology in the Tell Mozan surroundings. In: Deckers, K. (Ed.) Holocene landscapes through time in the Fertile Crescent. Brepols, Turnhout, 73-84. Deckers, K., Riehl, S. (2007) An evaluation of botanical assemblages from the 3rd to 2nd millennium BC in northeastern Syria. In: Kuzucuoğlu, C., Marro, C. (Eds.) Sociétés humaines et changement climatique à la fin du troisième millénaire: Une crise a-t-elle eu lieu en Haute Mésopotamie? Actes du colloque de Lyon. 5-8 décembre 2005, Varia Anatolica XIX. Institut français d´études anatoliennes Georges-Dumézil, Istanbul, 481-502.

Deckers, K., Riehl, S. (2008) Tells of the Upper Khabur: Their hydrological and agrarian contexts. Paléorient 34.2, 173-189.

de Gruchy, M., Deckers, K., Riehl, S. (2016) A Diachronic reconstruction of the northern Mesopotamian landscape (4th to 2nd Millennia BC) from three separate sources of evidence. Journal of Archaeological Science: Reports, 8, 250-267.

Doll, M. (2010) Meat, traction, wool: Urban livestock in Tell Mozan. In: Deckers, K., Doll, M, Pfälzner, P., Riehl, S. (eds.) Development of the Environment, Subsistence and settlement of the city of Urkes and its region. Studien zur Urbanisierung Nordmesopotamiens, Serie A 3. Harrassowitz, Wiesbaden, 191-360.

Dufraisse, A. (2006) Charcoal anatomy potential, wood diameter and radial growth. In: Dufraisse, A. (ed.) Charcoal analysis: New analytical tools and methods for archaeology. Papers from the table-ronde held in Basel 2004. Archaeopress, Oxford, 47-59.

Dufraisse, A., García Martínez, M.S. (2011) Mesurer les diamètres du bois de feu en anthracologie. Outils dendrométriques et interprétation des données. Anthropobotanica 2, 1-18.

Engel, T. (1993) Archaeobotanical analysis of timber and firewood used in the third millennium houses at Tall Bderi/Northeast Syria. In: Veenhof, K.R. (Ed.), Houses and Households. Nederlands Instituut voor het Nabije Oosten, Leiden, 105-113.

Finné, M., Woodbridge, J., Labuhn, I., Roberts, C.N. (2019) Holocene hydro-climatic variability in the Mediterranean: A synthetic multi-proxy reconstruction. The Holocene 29.5, 847-863.

Gaastra, J.S., Greenfield, T.L., Greenfield, H.J. (2020) There and back again: A zooarchaeological perspective on Early and Middle Bronze Age urbanism in the southern Levant. PLoS ONE 15(3): e0227255.

Gaastra, J.S., Welton, L., de Gruchy, M., Lawrence, D. (2021) Landscapes, climate and choice: Examining patterns in animal provisioning across the Near East c. 13,000-0 BCE. Quaternary International 1-44.

Griggs, C., DeGaetano, A., Kuniholm, P. I., und Newton, M. (2007) A regional high-frequency reconstruction of May-June precipitation in the north Aegean from oak tree rings, A.D. 1089-1989. International Journal of Climatology 27, 1075-1089.

Griggs, C., Manning, S. (2009) A reappraisal of the dendrochronology and dating of Tille Höyük (1993). Radiocarbon 51.2, 711-720.

Griggs, C., Manning, S.W., Kuniholm, P.I., Tarter, S.L. (2010-02-11) NOAA/WDS Paleoclimatology - Griggs - Tille Höyük - QUSP - ITRDB TURK043. NOAA National Centers for Environmental Information. https://doi.org/10.25921/32j1-am64. Accessed 09.06.2020.

Haneca K. (2005) Tree-ring analyses of European oak: implementation and relevance in (pre-)historical research in Flanders. Ph.D. dissertation, Ghent University, Ghent.

Henry, D.O., Cordova, C., Portillo, M., Albert, R.-M., De Witt, R., Emery-Barbier, A. (2016) Blame it on the goats? Desertification in the Near East during the Holocene. The Holocene, 1-13.

Hewett, Z., de Gruchy, M., Lawrence, D. (submitted) Raincheck: A new diachronic series of rainfall maps for Southwest Asia over the Holocene. Levant

Jones, M.D., Abu-Jaber, N., AlShdaifat, A., Baird, D., Cook, B.I., Cuthbert, M.O., Dean, J.R., Djamali, M., Eastwood, W., Fleitmann, D., Haywood, A., Kwiecien, O., Larsen, J., Maher, L.A., Metcalfe, S.E., Parker, A., Petrie, C.A., Primmer, N., Richter, T., Roberts, N., Roe, J., Tindall, J.C., Ünal-İmer, E., Weeks, L. (2019) 20,000 years of societal vulnerability and adaptation to climate change in southwest Asia. WIREs Water. 2019, 6:e1330.

Kabukcu, C. (2012) Early agriculture in northern Syria: Botanical remains from Jerablus Tahtani. Unpublished Master Thesis. University of Trent.Kabukcu, C. (2018) Identification of woodland management practices and tree growth conditions in archaeological fuel waste remains: a case study from the site of Çatalhöyük in central Anatolia, Turkey. Quaternary International 463 B, 282-297.

Kabukcu, C., Chabal, L. (2021) Sampling and quantitative analysis methods in anthracology from archaeological contexts: Achievements and prospects. Quaternary International 593-594. 9, 6-

18Kalayci, T. (2016) Settlement sizes and agricultural production territories: A remote sensing case study for the Early Bronze Age in Upper Mesopotamia, STAR: Science & Technology of Archaeological Research, 2.2, 217-234.

Kaniewski, D., Marriner, N., Cheddadi, R., Guiot, J., Van Campo, E. (2018) The 4.2 ka BP event in the Levant. Clim. Past, 14, 1529–1542.

Köchy, M., Mathaj, M., Jeltsch, F. et al. (2008) Resilience of stocking capacity to changing climate in arid to Mediterranean landscapes. Reg Environ Change 8, 73.

Kolinski, R. (2007) The Upper Khabur region in the second part of the third millennium BC. Altorientalische Forschungen 34, 1-28.

Lawrence, D., Palmisano, A., de Gruchy, M.W. (2021) Collapse and continuity: A multi-proxy reconstruction of settlement organization and population trajec0tories in the northern Fertile Crescent during the 4.2kya rapid climate change event. PLoS ONE 16(1): e0244871.

Lawrence, D., Rey, S. (2020) Extrapolating Ebla: Combining Remote Sensing, Survey and Textual Sources to Define an Early State. In: Lawrence, D., Philip, G., Altaweel, M. (eds.) New agendas in remote sensing and landscape archaeology in the Near East: Studies in honour of T.J. Wilkinson. Archaeopress, Oxford, 175-188.

Mason, S., Nesbitt, M. (2009) Acorns as food in southeast Turkey: Implications for prehistoric subsistence in southwest Asia. In: Fairbairn, A.S., Weiss, E. (eds.) From foragers to farmers. Papers in honour of Gordon C. Hillman. Oxbow books: Oxford and Oakville, 71-85.

Milano, L. (1995) Ebla: A third millennium city-state in ancient Syria. In Sasson, J. (Ed.) Civilizations of the ancient Near East, 2. Scribners/Macmillan, New York, 1219-1230.

Miller, N.F. (1997) Farming and herding along the Euphrates: Environmental constraint and cultural choices (fourth to second millennia B.C.). MASCA Research Papers in Science and Archaeology, 14 123-132.

Miller, N.F., Marston, J.M. (2012) Archaeological fuel remains as indicators of ancient west Asian agropastoral and land-use systems. Journal of Arid Environments 86, 97-103.

Moore, A.M.T, Hillman, G.C., Legge, A.J. (2000) Village on the Euphrates. Oxford University Press, Oxford.

Nelle, O. (2002) Charcoal burning remains and forest stand structure – Examples from the Black Forest (south-west-Germany) and the Bavarian Forest (south-east-Germany). In: Thiébault, S. (2002) Charcoal analysis. Methodological approaches, palaeoecological results and wood uses. Proceedings of the Second International Meeting of Anthracology, Paris, September 2000. Bar International Series 1063. Archaeopress, Oxford, 201-207.

Nicolescu, V.-N., Carvalho, J., Hochbichler, E., Bruckman, V., Piqué-Nicolau, M., Hernea, C., Viana, H., Štochlová, P., Ertekin, M., Tijardovic, M., Dubravac, T., Vandekerkhove, K., Kofman, P.D., Rossney, D., Unrau, A. (2017) Silvicultural Guidelines for European Coppice Forests. Albert Ludwig University Freiburg, Freiburg.

Palmisano, A., Lawrence, D., de Gruchy, M.W., Bevan, A., Shennan, S. (2021) Holocene regional population dynamics and climatic trends in the Near East: A first comparison using archaeo-demographic proxies. Quaternary Science Reviews 252, 106739.

Papachristou, T.G., Platis, P.D. (2011) The impact of cattle and goats grazing in oak stands of varying coppicing age. Acta Oecologica 37, 16-22.

Paradis-Grenouillet, S., Leleu, J.-P., Belingard, C., Rouaud, R., Allee, P. (2010) AnthracoLoJ. Un outil pur la simplification des measures dendrometriques. Collection EDYTEM11, 197-202.

Paradis-Grenouillet, S., Dufraisse, A., Allée, P. (2013) Radius of curvature measurements and wood diameter: a comparison of different image analysis techniques. In: Damblon, F. (Ed.) Proceedings of the Fourth International Meeting of Anthracology 2486. Bar International Series. Archaeopress, Oxford, 173-182.

Paradis-Grenouilet, S., Dufraisse, A. (2018) Deciduous oak/chestnut: Differential shrinkage of wood during charcoalification? Preliminary experimental results and implications for wood diameter study in anthracology. Quaternary International 463, 258-267.

Peltenburg, E. (1999) Jerablus-Tahtani 1992-6: a summary. In: del Olmo Lete, G. and Montero Fennollós, J.-L. (eds.) Archaeology of the Upper Syrian Euphrates. The Tishreen Dam area. Aula Orientalis-Supplementa 15, Editorial AUSA, Barcelona, 97-105.

Peltenburg, E. (2016) Carchemish in the 3rd millennium: A view from neighbouring Jerablus Tahtani. In: Wilkinson, T.J., Peltenburg, E. and Wilkinson, E.B. (eds.) Carchemish in context. The land of Carchemish project, 2006-2010. Oxbow Books, Oxford, 117-131.

Peltenburg, E., Wilkinson, T.J. (2008) Jerablus and the land of Carchemish: Excavation and survey in Syria. Current World Archaeology 27, 23-32.

Peña, L.P., Peña-Chocarro, L., Estévez, J.J.I., Urquijo, J.E.G. (2003) Ethnoarchaeology in the Moroccan Jebala (Western Rif): wood and dung as fuel, In: Neumann, K., Butler, A., Kahlheber, S. (eds.) Food, fuel and fields. Progress in African archaeobotany, Africa Praehistorica 15, 163-175.

Pessin, H. (2004) Stratégies d´approvisionnement et utilisation du bois dans le Moyen Euphrate et la Damascène. Approche antracologique comparative de sites historiques et préhistoriques. Ph.D. Thesis, University of Paris I, France.

Pessin, H. (2007) Analyses anthracologiques de deux sites du Moyen-Euphrate: Tilbeşar et Horum Höyük. Contribution à la problematique paléoclimatique de l´Holocène Moyen. In: Kuzucuoğlu, C., Marro, C. (eds.), Sociétés humaines et changement climatique à la fin du troisième millénaire: Une crise a-t-elle eu lieu en Haute Mésopotamie? Actes du colloque de Lyon, 5-8 décembre 2005. Varia Anatolica 19. Institut Français d´Etudes Anatoliennes-Georges Dumezil, Istanbul, 557-572.

Pfälzner, P. (2010) Introduction and synthesis: Urban development and ecology at Tell Mozan. In: Deckers, K., Doll, M., Pfälzner, P., Riehl, S. (eds.) Development of the environment, subsistence and settlement of the city of Urkes and its region. Studien zur Urbanisierung Nordmesopotamiens, Serie A 3. Harrassowitz, Wiesbaden, 1-12.

Pfälzner, P. (2012) The question of desurbanisation versus reurbanisation of the Syrian Jazirah in the late third and early second millennium BC. In: Laneri, N., Pfälzner, P. and Valentini, S. (eds.) Looking north. The socioeconomic dynamics of the northern Mesopotamian and Anatolian regions during the late third and early second millennium BC (Studien zur Urbanisierung Nordmesopotamiens. Ser. D, Supplementa 1). Harrassowitz, Wiesbaden, 51-80.

Price, M., Grossman, K., Paulette, T. (2017) Pigs and the pastoral bias: The other animal economy in northern Mesopotamia (3000-2000 BC). Journal of Anthropological Archaeology, 46-62.

Riehl, S. (2010) Plant production in a changing environment: the archaeobotanical remains from Tell Mozan. In: Deckers, K., Doll, M., Pfälzner, P., Riehl, S. (eds.) Development of the environment, subsistence and settlement of the city of Urkes and its region. Studien zur Urbanisierung Nordmesopotamiens. Harrassowitz, Wiesbaden, 13–158.

Riehl, S. (2019) Resource management at Tell el-Ábd. Economic specialization despite or because of environmental limitations? In: Finkbeiner, U. (Ed.) Final Reports of the Syrian-German Excavations at Tell el-'Abd, Volume III. Zaphon Verlag, 169-186.

Ristvet, L. (2007) Legal and archaeological territories of the second millennium BC in northern Mesopotamia. Antiquity 82, 317, 585-599.

Saito, L., Miller, W. W., Johnson, D. W., Qualls, R. G., Provencher, L., Carroll, E., et al. (2007) Fire effects on stable isotopes in a sierran forested watershed. J. Environ. Qual. 36, 91–100.

Salavert, A., Dufraisse, A. (2014) Understanding the impact of socio-economic activities on archaeological charcoal assemblages in temperate areas: A comparative analysis of firewood management in two Neolithic societies in Western Europe (Belgium, France). Journal of Anthropological Archaeology 35, 153–163.

Sallaberger, W. (2004) A note on the sheep and goat flocks – introduction to the texts. In: Milano, L., Sallaberger, W., Thalon, P., Van Lerberghe, K. (eds.) Third millennium cuneiform texts from Tell Beydar (seasons 1996-2002. Subartu XII. Brepols, Turnhout, 13-21.

Shahack-Gross, R., Finkelstein, I. (2008) Subsistence practices in an arid environment: A geoarchaeological investigation in an Iron Age site, the Negev Highlands, Israel. Journal of Archaeological Science 35, 965-982.

Schweingruber, F. H. (1993) Trees and wood in dendrochronology. Springer Series in Wood Science. Springer, Berlin, Heidelberg.

Schweingruber, F.H. (2001) Dendroökologische Holzanatomie. Anatomische Grundlagen der Dendrochronologie. Haupt, Wien.

Shafer, C.E, Blomo, V.J. (1980) Chapter 1: Agricultural trends, demand and pricing policy. In: Syria, Agricultural Sector Assessment, Band 4. Agricultural Marketing Annex, 1-71.

Smith, A., Proctor, L., Hart, T.C., Stein, G.J. (2019) The burning issue of dung in archaeobotanical samples: A case-study integrating macro-botanical remains, dung spherulites, and phytoliths to assess sample origin and fuel use at Tell Zeidan, Syria. Vegetation History and Archaeobotany 28,229-246.

Soltani, A., Eid, T., Hofstad, O. (2015) Optimizing management of goats and oak trees for sustainability and community´s welfare: a case study from Zagros, Iran. Scandinavian Journal of Forest Research 30.1, 49-59.

Speed, J.D.M., Austrheim, G., Hester, A.J., Mysterud, A. (2011) Browsing interacts with climate to determine tree-ring increment. Funct. Ecol. 25, 1018-1023.

Staubwasser, M., Weiss, H. (2006) Holocene climate and cultural evolution in late prehistoric-early historic west Asia. Quaternary Research 66, 372–387.

Styring, A.K., Charles, M., Fantone, F., Hald, M.M., McMahon, A., Meadow, R.H., Nicholls, G.K., Patel, A.K., Pitre, M.C., Smith, A., Soltysiak, A., Stein, G, Weber, J.A., Weiss, H., Bogaard, A. (2017) Isotope evidence for agricultural extensification reveals how the world´s first cities were fed. Nature Plants 3, 17076, 1-11.

Sweitzer, R.A., Van Vuren, D.H. (2002) Rooting and foraging effects of wild pigs on tree regeneration and acorn survival in California's oak woodland ecosystems. USDA Forest Service Gen. Tech. Rep. PSW-GTR-184, 19-231.

Tongo, A., Jalilvand, H., Hosseininasr, M., Naji, H. (2020) Variation in anatomical properties and hydraulic conductivity of Persian oak (*Quercus brantii* Lindl.) trees affected by dieback. Ecopersia 8.2, 117-124.

Trotter III, T.R., Cobb, N.S., Witham, T.G. (2002) Herbivory, plant resistance, and climate in the tree ring record: interactions distort climatic reconstructions. Proc. Natl. Acad.Sci. 23.99 (15) 10197-10202.

Ur, J. (2009) Emergent landscapes of movement in Early Bronze Age northern Mesopotamia. In: James, E., Erickson, C., Darling, W.A. (eds.) Landscapes of movement: Paths, trails, and roads in anthropological Perspective. University of Pennsylvania Museum Press, Philadelphia, 180-203.

Ur, J. (2010a) Cycles of civilization in northern Mesopotamia, 4400-2000 BC. Journal of Archaeological Research 18, 387-431.

Ur, J. (2010b) Landscapes of settlement and movement in northeastern Syria, https://doi.org/10.7910/DVN/NYWQO2, Harvard Dataverse, V2

Valipour, A., Plieninger, T., Shakeri, Z., Ghazanfari, H., Namiranian, M., Lexer, M.J. (2014) Traditional silvopastoral management and its effects on forest stand structure in northern Zagros, Iran. Forest Ecology and Management 327, 221-230.

Watson, P.J. (1979) Archaeological ethnography in Western Iran. Viking Fund. Publications in Anthropology 57. University of Arizona Press, Tucson.

Weiss, H., Courty, M.-A., Wetterstrom, W., Guichard, F., Senior, L., Meadow, R., Curnow, A. (1993) The genesis and collapse of third millennium north Mesopotamian civilization. Science 261, 995–1004.

Wick, L., Lemcke, G., Sturm, M. (2003) Evidence of Lateglacial and Holocene climatic change and human impact in Eastern Anatolia: High-Resolution pollen, charcoal, isotopic and geochemical records from the laminated sediments of Lake Van, Turkey. The Holocene 13.5, 665-675.

Wilkinson, T.J. (1989) Extensive sherd scatters and land-use intensity: Some recent results. Journal of Field Archaeology 16.1, 31-46.

Wilkinson, T.J. (1994) The structure and dynamics of dry-farming states in Upper Mesopotamia. Current Anthropology 35.5, 483-520.

Wilkinson, T. J. (1997) Environmental fluctuations, agricultural production and collapse: A view from Bronze Age Upper Mesopotamia. In: Dalfes, H. N., Kukla, G., Weiss, H. (eds.) Third millennium BC climate change and Old World collapse, Springer-Verlag, Berlin, 67–106.

Wilkinson, T.J. (2003) Archaeological landscapes of the Near East. Tucson. University of Arizona Press.

Wilkinson, T.J. (2004) On the Margin of the Euphrates: Settlement and Land Use at Tell es-Sweyhat and in the Upper Lake Assad Area, Syria. Oriental Institute Publications, vol. 124. The Oriental Institute, Chicago.

Wilkinson, T. J., Galiatsatos, N., Lawrence, D., Ricci, A., Dunford, R., Philip, G. (2012) Late Chalcolithic and Early Bronze Age landscapes of settlement and mobility in the Middle Euphrates: A reassessment. Levant 44.2, 139–185.

Wilkinson, T.J., French, C., Ur, J., Semple, M. (2010) The geoarchaeology of route systems in northern Syria. Geoarchaeology 25.6, 745 – 771.

Wilkinson, T. J., Tucker, D. J. (1995) Settlement development in the North Jazira, Iraq: A study of the archaeological landscape. Aris & Philips, Warminster.

Wilkinson, T.J., Philip, G., Bradbury, J., Dunford, R., Donaghue, D., Galiatsatos, N., Lawrence, D., Ricci, A., Smith, S.L. (2014) Contextualising early urbanization: Settlement cores, early states and agro-pastoral strategies in the Fertile Crescent during the fourth and third millennia BC. Journal of World Prehistory 27.1, 43-109.

Wilkinson, T.J., Deckers, K. (2015) 2. The regional Setting of Jerablus Tahtani. In: Peltenburg, E. et al. (eds.) Tell Jerablus Tahtani, Syria, I. Mortuary practices at an Early Bronze Age fort on the Euphrates River. Levant Supplementary Series 17. Oxbow, Oxford, 13-23.

Wilkinson, T.J., Peltenburg, E., McCartey, A., Wilkinson, E.B., Brown, M. (2007) Archaeology in the land of Carchemish: Landscape surveys in the area of Jerablus Tahtani, 2006. Levant 39, 213-247.

Willcox, G. (1999) Charcoal analysis and Holocene vegetation history in southern Syria. Quaternary Science Reviews 18, 711-716.

Wright, N. (2018) Examining dendrological features of oak as possible signals of systematic woodland management in the central Anatolian Bronze and Iron Ages. Quaternary International 463, 289-311.

Zeder, M. (1995) The archaeobiology of the Khabur Basin. Bull. Can. Soc. Mesop. Stud. 29, 21-32.

Zerboni, A., Nicoll, K. (2018) Enhanced zoogeomorphological processes in North Africa in the human-impacted landscapes of the Anthropocene. Geomorphology 331, 22–35.

Zohary, M. (1973) Geobotanical Foundations of the Middle East, 2 vol. Firscher, Stuttgart.

Site	Sample number (_3 stands for 3 measurements)	Stratigraphic layer in BC	Average diameter in cm	Standard deviation in mm	Average ring width	Measured annual rings	Approximate cambial age last annual ring	Method diameter measurement	Transversal max. measurements fragment	Context info
Mozan	MZ01_BP24_q0728b_3	2600-2300	2,4	5,8				trigonometry in an isocele triangle	7x4 mm	fill, A75, q728, Fs1228
Mozan	MZ01_BP30_q962b_3	2600-2300	1,7	1,9	1,01	6	9	trigonometry in a rectangle triangle	9x5 mm	dump, A85, q962, Fs1417
Mozan	MZ01_BP30a_3	2600-2300	1,2	0,6	1,08	3	6	trigonometry in an isocele triangle	7x8 mm	dump, A85, q962, Fs1417
Mozan	MZ01_BP30_q962_3	2600-2300	2,1	2,1	0,88	8	12	trigonometry in an isocele triangle	13x5 mm	dump, A85, q962, Fs1417
Mozan	MZ01 BP30 S1_4	2600-2300	9,3	18,3				trigonometry in a rectangle triangle	19x23 mm	dump, A85, q962, Fs1417
Mozan	MZ01 BP30 S2_2	2600-2300	3,7	1,2				trigonometry in a rectangle triangle	6x9 mm	dump, A85, q962, Fs1417
Mozan	MZ01_BP35_q1071b_3	2600-2300	4,1	2,4	0,38	14	53	trigonometry in an isocele triangle	6x5 mm	fill, A85, q1071, Fs1491
Mozan	MZ01_BP35_q1071e_3	2600-2300	1,9	0,8	0,36	7	26	trigonometry in an isocele triangle	5x3 mm	fill, A85, q1071, Fs1491
Mozan	MZ01_BP35_q1071f_3	2600-2300	7,8	87,9	0,47	3	82	trigonometry in an isocele triangle	3x4 mm	fill, A85, q1071, Fs1491
Mozan	MZ01_BP35_q1071a_3	2600-2300	11,5	0,7				trigonometry in a rectangle triangle	9x6 mm	fill, A85, q1071, Fs1491
Mozan	MZ01_BP35_3	2600-2300	27,5	47,6	0,49	9	278	trigonometry in an isocele triangle	8x5 mm	fill, A85, q1071, Fs1491
Mozan	MZ01 BP35 C2q1071 S1_2	2600-2300	11,6	23,1				trigonometry in a rectangle triangle	17x14 mm	fill, A85, q1071, Fs1491
Mozan	MZ01_BP37d_3	2600-2300	1,9	2,2	0,59	5	16	trigonometry in an isocele triangle	6x9 mm	fill/dump, A75, q1133, Fs1483
Mozan	MZ01_BP37_q1133_3	2600-2300	0,8	1,4	0,67	1	6	trigonometry in an isocele triangle	5x2 mm	fill/dump, A75, q1133, Fs1483
Mozan	MZ01_BP37_q1133b_3	2600-2300	2,2	8,2	1,06	1	11	trigonometry in a rectangle triangle	3x3 mm	fill/dump, A75, q1133, Fs1483
Mozan	MZ01_BP37_q1133e_3	2600-2300	3,5	3,8				trigonometry in an isocele triangle	4x3 mm	fill/dump, A75, q1133, Fs1483
Mozan	MZ01 BP37_2	2600-2300	0,8	1,0				trigonometry in a rectangle triangle		fill/dump, A75, q1133, Fs1483
Mozan	MZ01 BP37a_2	2600-2300	1,1	0,1				trigonometry in a rectangle triangle		fill/dump, A75, q1133, Fs1483
Mozan	MZ01 BP37 q1133 S1_2	2600-2300	3,3	2,1				trigonometry in a rectangle triangle	7x7 mm	fill/dump, A75, q1133, Fs1483
Mozan	MZ00 BP37	2600-2300			0,58	4				fill/dump, A75, q1133, Fs1483
Mozan	MZ01 BP37a	2600-2300			0,68	4				fill/dump, A75, q1133, Fs1483
Mozan	MZ01_q2893_3	2600-2300	2,9	2,0	0,69	7	21	trigonometry in an isocele triangle	10x8 mm	fill, A85, q2893, Fs1802
Mozan	MZ01_q2893b_3	2600-2300	2,5	1,0	0,79	6	16	trigonometry in an isocele triangle	5x6 mm	fill, A85, q2893, Fs1802
Mozan	MZ01_q2893c_3	2600-2300	3,6	8,2	0,62	5	29	trigonometry in an isocele triangle	4x6 mm	fill, A85, q2893, Fs1802
Mozan	MZ01_q2940_3	2600-2300	1,6	0,6				trigonometry in an isocele triangle	6x5 mm	fill, A85, q2940, Fs1802
Mozan	MZ01_q2940_3	2600-2300	2,6	2,1				trigonometry in a rectangle triangle		fill, A85, q2940, Fs1802
Mozan	MZ01_q2920_3	2600-2300	2,3	2,2	0,23	10	52	trigonometry in a rectangle triangle	4x5 mm	fill, A65/75/85, q2920, Fs1315
Mozan	MZ01_q2920b_3	2600-2300	2,1	1,7				trigonometry in an isocele triangle	4x4 mm	fill, A65/75/85, q2920, Fs1315
Mozan	MZ01_q2851a_3	2600-2300	25,9	51,8	0,42	1	306	trigonometry in an isocele triangle	11x10 mm	dump, A76, q2851, Fs2149
Mozan	MZ01_q2851_3	2600-2300	6,7	2,5	0,44	9	76	trigonometry in an isocele triangle	13x7 mm	dump, A76, q2851, Fs2149
Mozan	MZ01_q2851_3	2600-2300	1,2	0,8				trigonometry in an isocele triangle	15x8 mm	dump, A76, q2851, Fs2149
Mozan	MZ01_q2851d_3	2600-2300	4,2	6,8	0,27	9	78	trigonometry in an isocele triangle	6x5 mm	dump, A76, q2851, Fs2149
Mozan	MZ01_q2851e_3	2600-2300	5,6	4,1	0,34	7	82	trigonometry in an isocele triangle	7x8 mm	dump, A76, q2851, Fs2149
Mozan	MZ01_q2851b_3	2600-2300	7,6	7,1	0,44	14	86	trigonometry in a rectangle triangle	9x13 mm	dump, A76, q2851, Fs2149
Mozan	MZ01_q2851c_3	2600-2300	57,1	321,5	0,32	11	895	trigonometry in a rectangle triangle	5x5 mm	dump, A76, q2851, Fs2149
Mozan	MZ01_BP49b_3	2600-2300	2,4	6,4	0,48	5	25	trigonometry in a rectangle triangle	6x5 mm	floor accumulation in room, A75, q1797, Fs1640
Mozan	MZ01_BP49_3	2600-2300	2,2	1,1	0,60	5	19	trigonometry in an isocele triangle	7x6 mm	floor accumulation in room, A75, q1797, Fs1640
Mozan	MZ01 BP49_2	2600-2300	10,3	28,2				trigonometry in a rectangle triangle		floor accumulation in room, A75, q1797, Fs1640
Mozan	MZ01 BP49	2600-2300			0,26	11				floor accumulation in room, A75, q1797, Fs1640
Mozan	MZ01_q2914b_3	2600-2300	27,0	94,8	0,65	2	208	trigonometry in an isocele triangle	5x3 mm	dump, A85, q2914, Fs1885
Mozan	MZ01_q2908a_3	2600-2300	4,6	7,1	0,60	3	38	trigonometry in an isocele triangle	4x6 mm	dump, A85, q2908, Fs1827
Mozan	MZ01_q2908b_3	2600-2300	47,6	207,2	0,64	11	369	trigonometry in an isocele triangle	9x5 mm	dump, A85, q2908, Fs1827
Mozan	MZ01_q2908c_3	2600-2300	5,7	17,3	0,66	5	43	trigonometry in an isocele triangle	5x6 mm	dump, A85, q2908, Fs1827
Mozan	MZ01_q2908d_3	2600-2300	9,1	4,9	0,55	6	84	trigonometry in an isocele triangle	5x4 mm	dump, A85, q2908, Fs1827
Mozan	MZ01_q2908_3	2600-2300	3,1	3,8	0,53	6	29	trigonometry in an isocele triangle	6x3 mm	dump, A85, q2908, Fs1827
Mozan	MZ01_q2872c_3	2600-2300	5,8	6,5	0,29	16	100	trigonometry in an isocele triangle	6x6 mm	dump, A75/65, q2872, Fs1633
Mozan	MZ01_q2872b_3	2600-2300	0,9	0,7				trigonometry in an isocele triangle	8x8 mm	dump, A75/65, q2872, Fs1633
Mozan	MZ01_q2872d_3	2600-2300	5,7	7,0	0,23	3	126	trigonometry in an isocele triangle	6x5 mm	dump, A75/65, q2872, Fs1633
Mozan	MZ01_q2872e_3	2600-2300	1,8	0,3	0,31	6	30	trigonometry in an isocele triangle	5x5 mm	dump, A75/65, q2872, Fs1633
Mozan	MZ01_q2872f_3	2600-2300	11,5	16,2	0,18	6	316	trigonometry in an isocele triangle	6x4 mm	dump, A75/65, q2872, Fs1633
Mozan	MZ01 BP40_2	2600-2300	6,2	6,2				trigonometry in a rectangle triangle		dump, A75, q1488, Fs1633
Mozan	MZ01 BP40a_2	2600-2300	12,0	10,1				trigonometry in a rectangle triangle		dump, A75, q1488, Fs1633
Mozan	MZ01 BP40 S1_2	2600-2300	2,8	0,7				trigonometry in a rectangle triangle	4x2 mm	dump, A75, q1488, Fs1633
Mozan	MZ01 BP40a	2600-2300			0,63	4				dump, A75, q1488, Fs1633
Mozan	MZ01_q2866c_3	2600-2300	23,8	45,9	0,60	7	199	trigonometry in an isocele triangle	7x10 mm	fill, A65, q2866, Fs1315
Mozan	MZ01_q2866d_3	2600-2300	4,1	3,6	0,33	8	64	trigonometry in an isocele triangle	4x4 mm	fill, A65, q2866, Fs1315
Mozan	MZ01_q2866a_3	2600-2300	143,4	362,6	0,28	9		trigonometry in a rectangle triangle	5x6 mm	fill, A65, q2866, Fs1315
Mozan	MZ01_q2865c_3	2600-2300	5,2	5,7	0,70	7	37	trigonometry in an isocele triangle	8x5 mm	dump in courtyard, A75, q2865, Fs2179
Mozan	MZ01_q2865j_3	2600-2300	3,0	9,9	0,94	3	16	trigonometry in an isocele triangle	5x3 mm	dump in courtyard, A75, q2865, Fs2179
Mozan	MZ01_q2865d_3	2600-2300	6,9	6,2	0,62	8	56	trigonometry in an isocele triangle	11x9 mm	dump in courtyard, A75, q2865, Fs2179
Mozan	MZ01_q2865e_3	2600-2300	3,8	5,4	0,77	14	25	trigonometry in an isocele triangle	12x11 mm	dump in courtyard, A75, q2865, Fs2179
Mozan	MZ01_q2865f_3	2600-2300	7,0	9,8	0,38	8	93	trigonometry in an isocele triangle	4x8 mm	dump in courtyard, A75, q2865, Fs2179
Mozan	MZ01_q2865g_3	2600-2300	11,4	114,7	1,82	2	31	trigonometry in an isocele triangle	5x6 mm	dump in courtyard, A75, q2865, Fs2179
Mozan	MZ01_q2865b_3	2600-2300	6,1	42,7	0,44	14	68	trigonometry in a rectangle triangle	8x7 mm	dump in courtyard, A75, q2865, Fs2179
Mozan	MZ01_q2860a_3	2600-2300	2,1	1,1	0,50	9	21	trigonometry in an isocele triangle	7x6 mm	dump, A75, q2860, Fs1632
Mozan	MZ01_q2860b_3	2600-2300	3,9	8,0	0,93	10	21	trigonometry in an isocele triangle	12x9 mm	dump, A75, q2860, Fs1632
Mozan	MZ01_q2860j_3	2600-2300	0,7	2,6	0,31	10	12	trigonometry in an isocele triangle	4x5 mm	dump, A75, q2860, Fs1632
Mozan	MZ01_q2860i_3	2600-2300	2,0	0,7	1,19	2	8	trigonometry in an isocele triangle	4x7 mm	dump, A75, q2860, Fs1632
Mozan	MZ01_q2860k_3	2600-2300	3,9	3,5	0,43	7	45	trigonometry in an isocele triangle	4x6 mm	dump, A75, q2860, Fs1632
Mozan	MZ01_q2860h_3	2600-2300	28,5	43,8	1,19	2	120	trigonometry in an isocele triangle	5x8 mm	dump, A75, q2860, Fs1632
Mozan	MZ01_q2860e_3	2600-2300	2,2	2,4	0,47	6	23	trigonometry in an isocele triangle	5x7 mm	dump, A75, q2860, Fs1632
Mozan	MZ01_q2860e_3	2600-2300	0,6	0,4				trigonometry in an isocele triangle	5x8 mm	dump, A75, q2860, Fs1632
Mozan	MZ01_q2860c_3	2600-2300	2,7	1,5	0,45	10	30	trigonometry in an isocele triangle	6x5 mm	dump, A75, q2860, Fs1632
Mozan	MZ01_q2860l_3	2600-2300	0,7	0,2	0,22	8	16	trigonometry in an isocele triangle	4x7 mm	dump, A75, q2860, Fs1632
Mozan	MZ01_q2860m_3	2600-2300	5,1	1,6	0,43	6	60	trigonometry in an isocele triangle	4x4 mm	dump, A75, q2860, Fs1632
Mozan	MZ01_q2860n_3	2600-2300	3,8	2,3	0,33	10	57	trigonometry in an isocele triangle	5x4 mm	dump, A75, q2860, Fs1632
Mozan	MZ01_q2860q_3	2600-2300	6,6	22,6				trigonometry in an isocele triangle	4x11 mm	dump, A75, q2860, Fs1632
Mozan	MZ01_q2860r_3	2600-2300	4,3	7,7	0,76	2	29	trigonometry in an isocele triangle	4x6 mm	dump, A75, q2860, Fs1632
Mozan	MZ01_q2860f_3	2600-2300	6,0	26,9	0,54	16	56	trigonometry in a rectangle triangle	10x7mm	dump, A75, q2860, Fs1632
Mozan	MZ01_q2860g_3	2600-2300	1,0	0,1				circle tool	5x10 mm	dump, A75, q2860, Fs1632
Mozan	MZ01_q2854b_3	2600-2300	10,6	52,9	0,70	6	76	trigonometry in an isocele triangle	6x4 mm	on floor, A75, q2854, Fs1682
Mozan	MZ01_q2854a_3	2600-2300	8,1	64,6	1,07	5	38	trigonometry in a rectangle triangle	5x4 mm	on floor, A75, q2854, Fs1682
Mozan	MZ00_q0565e_3	2600-2300	2,6	10,3	0,50	6	26	trigonometry in an isocele triangle	4x3 mm	dump between floors in open area, A84/A85, q565, Fs621
Mozan	MZ00_q0565d_3	2600-2300	2,9	4,6	0,60	2	24	trigonometry in an isocele triangle	3x6 mm	dump between floors in open area, A84/A85, q565, Fs621
Mozan	MZ00_q565b_3	2600-2300	1,1	0,3	0,48	5	11	trigonometry in an isocele triangle	4x3 mm	dump between floors in open area, A84/A85, q565, Fs621
Mozan	MZ00_q565e_3	2600-2300	3,5	6,0	0,62	3	28	trigonometry in an isocele triangle	4x4 mm	dump between floors in open area, A84/A85, q565, Fs621
Mozan	MZ00_q0565c_3	2600-2300	7,4	6,4	1,29	3	29	trigonometry in an isocele triangle	6x3 mm	dump between floors in open area, A84/A85, q565, Fs621
Mozan	MZ00_q0565a_3	2600-2300	4,8	7,8	0,25	15	94	trigonometry in a rectangle triangle	7x9 mm	dump between floors in open area, A84/A85, q565, Fs621
Mozan	MZ00_q0565b_3	2600-2300	5,5	8,7				trigonometry in a rectangle triangle	6x5 mm	dump between floors in open area, A84/A85, q565, Fs621
Mozan	MZ00_q565a_3	2600-2300	2,9	1,7	0,28	9	51	trigonometry in a rectangle triangle	6x4 mm	dump between floors in open area, A84/A85, q565, Fs621
Mozan	MZ00_q565c_3	2600-2300	1,4	1,9	0,47	4	15	trigonometry in a rectangle triangle	3x4 mm	dump between floors in open area, A84/A85, q565, Fs621
Mozan	MZ00_q565d_3	2600-2300	6,4	5,9	0,51	3	63	trigonometry in a rectangle triangle	5x5mm	dump between floors in open area, A84/A85, q565, Fs621
Mozan	MZ01-q2853_2	2600-2300	10,2	28,0				trigonometry in a rectangle triangle		dump, A75, q2853, Fs1638
Mozan	MZ01 q2850 S1_2	2600-2300	4,8	2,9				trigonometry in a rectangle triangle	10x10 mm	fill in room, A75, q2850, Fs1683
Mozan	MZ01 q2850 S2_2	2600-2300	13,2	28,1				trigonometry in a rectangle triangle	7x9 mm	fill in room, A75, q2850, Fs1683
Mozan	MZ01 q2850 S3_2	2600-2300	6,9	3,8				trigonometry in a rectangle triangle	8x12 mm	fill in room, A75, q2850, Fs1683
Mozan	MZ01 q2850 S4_2	2600-2300	29,0	2,3				trigonometry in a rectangle triangle	28x17 mm	fill in room, A75, q2850, Fs1683
Mozan	MZ01 BP58 S1_2	2600-2300	5,9	4,1				trigonometry in a rectangle triangle	3x5 mm	fill on street, A75/A85, q2360, Fs1908
Mozan	MZ01 BP58 S2_2	2600-2300	1,9	4,8				trigonometry in a rectangle triangle	4x2 mm	fill on street, A75/A85, q2360, Fs1908
Mozan	MZ01 BP58 S3_2	2600-2300	5,9	10,3				trigonometry in a rectangle triangle	3x2 mm	fill on street, A75/A85, q2360, Fs1908

Mozan	MZ01 q2891_S1_2	2600-2300	3,7	3,8				trigonometry in a rectangle triangle	6x5 mm	dump, A85, q2891, Fs1827
Mozan	MZ01 q2891_S3_2	2600-2300	5,5	5,9				trigonometry in a rectangle triangle	4x4 mm	dump, A85, q2891, Fs1827
Mozan	MZ01 q2929 Fs 1951 S2_2	2600-2300	3,6	7,5				trigonometry in a rectangle triangle	5x9 mm	dump, A95, q2929, Fs1951
Mozan	MZ01 q2929 Fs 1951 S3_2	2600-2300	8,4	14,5				trigonometry in a rectangle triangle	3x4 mm	dump, A95, q2929, Fs1951
Mozan	MZ01 q2882 S1_2	2600-2300	3,7	1,3				trigonometry in a rectangle triangle	4x4 mm	fill, A85/A75, q2882, Fs1879
Mozan	MZ01 q2882 S2_2	2600-2300	9,5	9,2				trigonometry in a rectangle triangle	6x4 mm	fill, A85/A75, q2882, Fs1879
Mozan	MZ01 q2882 S3_2	2600-2300	5,8	15,0				trigonometry in a rectangle triangle	4x3 mm	fill, A85/A75, q2882, Fs1879
Mozan	MZ01 q2882 S4_2	2600-2300	13,7	7,4				trigonometry in a rectangle triangle	4x8 mm	fill, A85/A75, q2882, Fs1879
Mozan	MZ01 q2906 S1_2	2600-2300	13,8	10,6				trigonometry in a rectangle triangle	4x4 mm	accumulation on floor in open area, A85, q2906, Fs2021
Mozan	MZ01 q2906 S2_2	2600-2300	6,8	0,9				trigonometry in a rectangle triangle	4x4 mm	accumulation on floor in open area, A85, q2906, Fs2021
Mozan	MZ01 q2903 S2_2	2600-2300	1,0	0,5				trigonometry in a rectangle triangle	3x5 mm	dump, A85, q2906, Fs2021
Mozan	MZ01 q2903 S3_2	2600-2300	5,9	3,8				trigonometry in a rectangle triangle	3x4 mm	dump, A85, q2906, Fs2021
Mozan	MZ01_q601_3	2600-2300	1,5	3,8	0,51	4	15	trigonometry in an isocele triangle	3x5 mm	dump, A75, q601, Fs1223
Mozan	MZ00 BP37 q1357 S1_2	2300-2100	4,2	3,7				trigonometry in a rectangle triangle	7x10 mm	pit fill, A95, q1357, Fs732
Mozan	MZ00 BP37 q1357 S2_2	2300-2100	5,0	5,2				trigonometry in a rectangle triangle	5x5 mm	pit fill, A95, q1357, Fs732
Mozan	MZ00 BP37 q1357 S3_2	2300-2100	5,7	18,0				trigonometry in a rectangle triangle	5x4 mm	pit fill, A95, q1357, Fs732
Mozan	MZ00 BP37 q1357 S4_2	2300-2100	6,0	2,3				trigonometry in a rectangle triangle	4x6 mm	pit fill, A95, q1357, Fs732
Mozan	MZ00 BP37 q1357 S5_2	2300-2100	4,3	5,5				trigonometry in a rectangle triangle	7x6 mm	pit fill, A95, q1357, Fs732
Mozan	MZ00 BP37 q1357 S6b_2	2300-2100	10,5	10,2				trigonometry in a rectangle triangle	7x10 mm	pit fill, A95, q1357, Fs732
Mozan	MZ00 BP37 q1357 S9_2	2300-2100	7,7	25,3				trigonometry in a rectangle triangle	5x4 mm	pit fill, A95, q1357, Fs732
Mozan	MZ00 BP37 q1357 S10_2	2300-2100	7,0	3,8				trigonometry in a rectangle triangle	7x4 mm	pit fill, A95, q1357, Fs732
Mozan	MZ00 BP37 q1357 S11_2	2300-2100	2,5	1,6				trigonometry in a rectangle triangle	3x7 mm	pit fill, A95, q1357, Fs732
Mozan	MZ00 BP37 q1357 S12_2	2300-2100	8,5	6,0				trigonometry in a rectangle triangle	8x4 mm	pit fill, A95, q1357, Fs732
Mozan	MZ00 BP37 q1357 S13_2	2300-2100	6,3	3,4				trigonometry in a rectangle triangle	5x3 mm	pit fill, A95, q1357, Fs732
Mozan	MZ00 BP37 q1357 S14_2	2300-2100	5,7	5,6				trigonometry in a rectangle triangle	4x3 mm	pit fill, A95, q1357, Fs732
Mozan	MZ00 BP37 q1357 S15_2	2300-2100	4,9	2,0				trigonometry in a rectangle triangle	5x3 mm	pit fill, A95, q1357, Fs732
Mozan	MZ 00 BP37b_2	2300-2100	3,1	11,7				trigonometry in a rectangle triangle	4x6 mm	pit fill, A95, q1357, Fs732
Mozan	MZ00_BP37d_3	2300-2100	9,6	48,2	1,18	1	41	trigonometry in an isocele triangle	5x3 mm	pit fill, A95, q1357, Fs732
Mozan	MZ00_BP37t_3	2300-2100	0,9	2,6	0,78	4	6	trigonometry in an isocele triangle	5x4 mm	pit fill, A95, q1357, Fs732
Mozan	MZ00_BP37_q1357_3	2300-2100	0,8	0,1	0,58	4	6	trigonometry in an isocele triangle	6 x 6 mm	pit fill, A95, q1357, Fs732
Mozan	MZ00_BP37_q1357a_3	2300-2100	2,5	14,0	0,43	6	29	trigonometry in an isocele triangle	4x3 mm	pit fill, A95, q1357, Fs732
Mozan	MZ00_BP37_q1357b_3	2300-2100	0,7	0,4				trigonometry in an isocele triangle	5x3 mm	pit fill, A95, q1357, Fs732
Mozan	MZ00_BP37c_3	2300-2100	2,6	1,4	0,41	11	31	trigonometry in an isocele triangle	7x3mm	pit fill, A95, q1357, Fs732
Mozan	MZ00_BP37f_3	2300-2100	3,6	19,3	0,40	6	45	trigonometry in an isocele triangle	4x3 mm	pit fill, A95, q1357, Fs732
Mozan	MZ00_BP37g_3	2300-2100	7,2	31,4	0,66	4	55	trigonometry in an isocele triangle	5x3 mm	pit fill, A95, q1357, Fs732
Mozan	MZ00_BP37i_3	2300-2100	1,5	4,3				trigonometry in an isocele triangle		pit fill, A95, q1357, Fs732
Mozan	MZ00_BP37n_3	2300-2100	5,1	13,7	0,94	1	27	trigonometry in an isocele triangle	5x3 mm	pit fill, A95, q1357, Fs732
Mozan	MZ00_BP37m_3	2300-2100	1,6	1,5	1,46	1	6	trigonometry in an isocele triangle	5x5mm	pit fill, A95, q1357, Fs732
Mozan	MZ00_BP37l_3	2300-2100	5,8	34,6	1,08	1	27	trigonometry in an isocele triangle	4x4 mm	pit fill, A95, q1357, Fs732
Mozan	MZ00_BP37o_3	2300-2100	1,9	6,6	0,42	8	22	trigonometry in an isocele triangle	6x6 mm	pit fill, A95, q1357, Fs732
Mozan	MZ00_BP37p_3	2300-2100	4,4	3,4	0,49	2	45	trigonometry in an isocele triangle	5x2 mm	pit fill, A95, q1357, Fs732
Mozan	MZ01_BP62e_3	2300-2100	1,4	0,6	0,24	2	29	trigonometry in an isocele triangle	4x5 mm	dump in room, A74, q2615, Fs2083
Mozan	MZ01_BP62f_3	2300-2100	1,2	5,6				trigonometry in an isocele triangle	3x3 mm	dump in room, A74, q2615, Fs2083
Mozan	MZ01_BP62h_3	2300-2100	1,1	0,8	0,49	4	12	trigonometry in an isocele triangle	6x5 mm	dump in room, A74, q2615, Fs2083
Mozan	MZ01_BP62i_3	2300-2100	1,3	0,3	0,40	9	17	trigonometry in an isocele triangle	5x5 mm	dump in room, A74, q2615, Fs2083
Mozan	MZ01_BP62c_3	2300-2100	1,2	4,6				trigonometry in an isocele triangle	4x5 mm	dump in room, A74, q2615, Fs2083
Mozan	MZ01_BP62a_3	2300-2100	0,7	1,3	2,19	1	2	trigonometry in an isocele triangle	6x7 mm	dump in room, A74, q2615, Fs2083
Mozan	MZ01_BP62w_3	2300-2100	5,8	20,4				trigonometry in an isocele triangle	4x4 mm	dump in room, A74, q2615, Fs2083
Mozan	MZ01_BP62v_3	2300-2100	2,7	7,9	0,30	7	45	trigonometry in an isocele triangle	3x6 mm	dump in room, A74, q2615, Fs2083
Mozan	MZ01_BP62s_3	2300-2100	1,1	2,7	1,93	2	3	trigonometry in an isocele triangle	7x3mm	dump in room, A74, q2615, Fs2083
Mozan	MZ01_BP62r_3	2300-2100	2,7	0,5	0,41	11	32	trigonometry in an isocele triangle	5x2 mm	dump in room, A74, q2615, Fs2083
Mozan	MZ01_BP62p_3	2300-2100	1,4	0,8	0,47	6	15	trigonometry in an isocele triangle	4x4 mm	dump in room, A74, q2615, Fs2083
Mozan	MZ01_BP62q_3	2300-2100	4,8	7,6	0,36	14	68	trigonometry in an isocele triangle	6x3 mm	dump in room, A74, q2615, Fs2083
Mozan	MZ01_BP62o_3	2300-2100	1,7	0,8	0,29	9	28	trigonometry in an isocele triangle	4x4 mm	dump in room, A74, q2615, Fs2083
Mozan	MZ01_BP62m_3	2300-2100	1,1	3,1				trigonometry in an isocele triangle	4x4 mm	dump in room, A74, q2615, Fs2083
Mozan	MZ01_BP62y_3	2300-2100	0,8	0,9	0,74	1	5	trigonometry in an isocele triangle	3x3 mm	dump in room, A74, q2615, Fs2083
Mozan	MZ01_BP62z_3	2300-2100	2,5	1,6	0,20	6	65	trigonometry in an isocele triangle	2x3 mm	dump in room, A74, q2615, Fs2083
Mozan	MZ01_BP62aa_3	2300-2100	1,0	0,3				trigonometry in an isocele triangle	5x4 mm	dump in room, A74, q2615, Fs2083
Mozan	MZ01_BP62ad_3	2300-2100	1,4	2,6				trigonometry in an isocele triangle	5x4 mm	dump in room, A74, q2615, Fs2083
Mozan	MZ01_BP62g_3	2300-2100	4,7	16,0	0,33	3	72	trigonometry in a rectangle triangle	5x2 mm	dump in room, A74, q2615, Fs2083
Mozan	MZ01_BP62d_3	2300-2100	1,6	0,4	0,42	8	19	trigonometry in a rectangle triangle	5x6 mm	dump in room, A74, q2615, Fs2083
Mozan	MZ01_BP62b_3	2300-2100	1,7	8,1	0,39	6	22	trigonometry in a rectangle triangle	4x5 mm	dump in room, A74, q2615, Fs2083
Mozan	MZ01 BP62 S1_2	2300-2100	4,4	2,1				trigonometry in a rectangle triangle	10x11 mm	dump in room, A74, q2615, Fs2083
Mozan	MZ01 BP62 S2_2	2300-2100	2,9	10,3				trigonometry in a rectangle triangle	7x4 mm	dump in room, A74, q2615, Fs2083
Mozan	MZ01 BP62 S3_2	2300-2100	1,3	0,5				trigonometry in a rectangle triangle	5x6 mm	dump in room, A74, q2615, Fs2083
Mozan	MZ01 BP62 S4_2	2300-2100	2,6	10,0				trigonometry in a rectangle triangle	5x4 mm	dump in room, A74, q2615, Fs2083
Mozan	MZ01 BP62 S5_2	2300-2100	2,3	1,2				trigonometry in a rectangle triangle	5x3 mm	dump in room, A74, q2615, Fs2083
Mozan	MZ01 BP62 S6_2	2300-2100	2,9	7,7				trigonometry in a rectangle triangle	3x6 mm	dump in room, A74, q2615, Fs2083
Mozan	MZ01 BP62 S7_2	2300-2100	2,9	4,8				trigonometry in a rectangle triangle	5x5 mm	dump in room, A74, q2615, Fs2083
Mozan	MZ01 BP62	2300-2100			0,41	11				dump in room, A74, q2615, Fs2083
Mozan	MZ01_BP60b_3	2300-2100	1,3	1,9				trigonometry in an isocele triangle	3x5 mm	pit fill, A74, q2544, Fs2081
Mozan	MZ01_BP60e_3	2300-2100	1,3	0,5				trigonometry in a rectangle triangle	3x3 mm	pit fill, A74, q2544, Fs2081
Mozan	MZ01_BP60a_3	2300-2100	2,2	1,6	1,54	2	7	trigonometry in an isocele triangle	5x3 mm	pit fill, A74, q2544, Fs2081
Mozan	MZ01 BP60_2	2300-2100	3,7	4,6				trigonometry in a rectangle triangle		pit fill, A74, q2544, Fs2081
Mozan	MZ01 BP60a_2	2300-2100	2,6	5,4				trigonometry in a rectangle triangle		pit fill, A74, q2544, Fs2081
Mozan	MZ01_BP67_3	2300-2100	19,9	95,1	1,09	3	91	trigonometry in an isocele triangle	4x3 mm	ash around tannur in courtyard, A74, q2266, Fs1971
Mozan	MZ01_BP67b_3	2300-2100	4,0	5,3	0,31	5	64	trigonometry in an isocele triangle	2x2 mm	ash around tannur in courtyard, A74, q2266, Fs1971
Mozan	MZ01 BP67 S1_2	2300-2100	9,9	8,1				trigonometry in a rectangle triangle	8x8 mm	ash around tannur in courtyard, A74, q2266, Fs1971
Mozan	MZ01 BP67 S2_2	2300-2100	9,7	10,5				trigonometry in a rectangle triangle	8x7 mm	ash around tannur in courtyard, A74, q2266, Fs1971
Mozan	MZ01 BP67 S3_2	2300-2100	6,2	6,6				trigonometry in a rectangle triangle	5x8 mm	ash around tannur in courtyard, A74, q2266, Fs1971
Mozan	MZ01 BP67 S4_2	2300-2100	4,9	5,9				trigonometry in a rectangle triangle	6x4 mm	ash around tannur in courtyard, A74, q2266, Fs1971
Mozan	MZ01 BP67a	2300-2100			0,37	8				ash around tannur in courtyard, A74, q2266, Fs1971
Mozan	MZ01 BP67b	2300-2100			0,29	15				ash around tannur in courtyard, A74, q2266, Fs1971
Mozan	MZ01_BP59a_3	2300-2100	4,4	5,2	0,49	6	45	trigonometry in an isocele triangle	4x5 mm	pit fill, A74, q2543, Fs2081
Mozan	MZ01_BP59c_3	2300-2100	10,5	53,7	0,40	6	132	trigonometry in an isocele triangle	4x4 mm	pit fill, A74, q2543, Fs2081
Mozan	MZ01_BP59b_3	2300-2100	39,3	540,0	0,44	6	449	trigonometry in a rectangle triangle	4x5 mm	pit fill, A74, q2543, Fs2081
Mozan	MZ01 BP59 S1_2	2300-2100	9,2	15,4				trigonometry in a rectangle triangle	12x11 mm	pit fill, A74, q2543, Fs2081
Mozan	MZ01 BP59 S2_2	2300-2100	2,6	1,0				trigonometry in a rectangle triangle	5x3 mm	pit fill, A74, q2543, Fs2081
Mozan	MZ01 BP59 S3_2	2300-2100	6,3	14,6				trigonometry in a rectangle triangle	6x6 mm	pit fill, A74, q2543, Fs2081
Mozan	MZ01 BP59 S4_2	2300-2100	3,8	3,6				trigonometry in a rectangle triangle	4x3 mm	pit fill, A74, q2543, Fs2081
Mozan	MZ01 BP59 S5_2	2300-2100	2,8	1,5				trigonometry in a rectangle triangle	4x4 mm	pit fill, A74, q2543, Fs2081
Mozan	MZ01 BP59 S6_2	2300-2100	3,3	7,3				trigonometry in a rectangle triangle	3x3 mm	pit fill, A74, q2543, Fs2081
Mozan	MZ01 BP59 S7_2	2300-2100	4,0	5,3				trigonometry in a rectangle triangle	3x3 mm	pit fill, A74, q2543, Fs2081
Mozan	MZ01_BP50_3	2300-2100	0,8	1,1				trigonometry in an isocele triangle	4x5 mm	pit fill in room, A74, q2002, Fs1852
Mozan	MZ01_q295b_3	2300-2100	2,1	3,1				trigonometry in an isocele triangle	7x4 mm	dump in open area, A85, q295, Fs0513
Mozan	MZ00_q0295a_3	2300-2100	4,0	2,0	0,26	13	79	trigonometry in an isocele triangle	7x5 mm	dump in open area, A85, q295, Fs0513
Mozan	MZ00_q0295b_3	2300-2100	16,8	59,8				trigonometry in an isocele triangle	8x7 mm	dump in open area, A85, q295, Fs0513
Mozan	MZ01_q2913_3	2300-2100	4,1	12,2				trigonometry in an isocele triangle	4x6 mm	dump, A85, q2913, Fs1419
Mozan	MZ01_q2913b_3	2300-2100	3,5	6,5	0,37	7	47	trigonometry in an isocele triangle	5x5 mm	dump, A85, q2913, Fs1419
Mozan	MZ00_q0342c_4	2300-2100	7,9	6,7	0,89	7	44	trigonometry in a rectangle triangle	10x10 mm	dump in open area, A84/A85, q342, Fs0517
Mozan	MZ00_q0342b_3	2300-2100	3,4	1,8	0,60	5	28	trigonometry in an isocele triangle	7x5 mm	dump in open area, A84/A85, q342, Fs0517
Mozan	MZ01_q2858a_3	2300-2100	3,9	4,3	0,35	8	55	trigonometry in a rectangle triangle	4x7 mm	dump, A75, q2858, Fs1382
Mozan	MZ01 C2 q0728 Querc. S1_2	2300-2100	6,4	9,4				trigonometry in a rectangle triangle	8x5 mm	dump, A75, q728, Fs1228
Mozan	MZ01 q2888 Fs1497 S1_2	2300-2100	3,9	2,5				trigonometry in a rectangle triangle	4x5 mm	dump/fill, q2888, Fs1497
Mozan	MZ01 q2888 Fs1497 S2_2	2300-2100	4,4	15,4				trigonometry in a rectangle triangle	6x3 mm	dump/fill, q2888, Fs1497
Mozan	MZ01 q2912 S1_2	2300-2100	7,0	6,2				trigonometry in a rectangle triangle	13x6 mm	fill, A85, q2912, Fs1426
Mozan	MZ01 q2912 S2_2	2300-2100	7,9	11,8				trigonometry in a rectangle triangle	6x8 mm	fill, A85, q2912, Fs1426
Mozan	MZ01 q2912 S3_2	2300-2100	5,7	12,4				trigonometry in a rectangle triangle	6x8mm	fill, A85, q2912, Fs1426
Mozan	MZ01 q2912 S4_2	2300-2100	4,3	4,1				trigonometry in a rectangle triangle	6x7 mm	fill, A85, q2912, Fs1426

Mozan	MZ01 q2912 S5_2	2300-2100	6,3	3,4				trigonometry in a rectangle triangle	7x8 mm	fill, A85, q2912, Fs1426
Mozan	MZ01 q2614 S1_2	2300-2100	3,0	0,1				trigonometry in a rectangle triangle	7x9 mm	brickfall, A74, q2614, Fs2087
Mozan	MZ01 q2614 S2_2	2300-2100	2,6	2,4				trigonometry in a rectangle triangle	6x7 mm	brickfall, A74, q2614, Fs2087
Mozan	MZ01 q2614 S3_2	2300-2100	2,9	1,5				trigonometry in a rectangle triangle	6x8 mm	brickfall, A74, q2614, Fs2087
Mozan	MZ01 q2614 S4_2	2300-2100	2,1	0,7				trigonometry in a rectangle triangle	4x5 mm	brickfall, A74, q2614, Fs2087
Mozan	MZ01 q2614 S5_2	2300-2100	1,4	3,4				trigonometry in a rectangle triangle	2x3 mm	brickfall, A74, q2614, Fs2087
Mozan	MZ01 q2304 S2_2	2300-2100	6,6	1,3				trigonometry in a rectangle triangle	5x3 mm	on floor in room, A73, q2304, Fs1832
Mozan	MZ01 q2304 S3_2	2300-2100	7,3	7,3				trigonometry in a rectangle triangle	4x2 mm	on floor in room, A73, q2304, Fs1832
Mozan	MZ99_BP58_3	2100-2000	1,1	1,4	0,34	10	16	trigonometry in an isocele triangle	4x7 mm	fill of room, A94, q423, Fs206
Mozan	MZ99_BP58d_3	2100-2000	2,3	1,2	0,40	14	29	trigonometry in an isocele triangle	7x5 mm	fill of room, A94, q423, Fs206
Mozan	MZ99_BP58e_3	2100-2000	4,4	11,6	0,48	6	45	trigonometry in an isocele triangle	4x5 mm	fill of room, A94, q423, Fs206
Mozan	MZ99_BP58g_3	2100-2000	4,0	1,5	0,34	5	58	trigonometry in an isocele triangle	3x3 mm	fill of room, A94, q423, Fs206
Mozan	MZ99_BP58b_3	2100-2000	9,0	26,0	0,37	7	120	trigonometry in a rectangle triangle	6x6 mm	fill of room, A94, q423, Fs206
Mozan	MZ99_BP58c_3	2100-2000	0,8	1,3	0,26	9	16	trigonometry in a rectangle triangle	5x5 mm	fill of room, A94, q423, Fs206
Mozan	MZ99_BP58f_3	2100-2000	1,7	0,8	0,35	6	24	trigonometry in a rectangle triangle	3x5 mm	fill of room, A94, q423, Fs206
Mozan	MZ99_BP51c_4	2100-2000	4,0	24,5	0,32	8	64	trigonometry in an isocele triangle	6x4 mm	fill of room, A94, q433, Fs206
Mozan	MZ99_BP51d_3	2100-2000	1,5	1,8	0,33	6	23	trigonometry in an isocele triangle	4x3 mm	fill of room, A94, q433, Fs206
Mozan	MZ99 BP51c_2	2100-2000	7,9	3,7				trigonometry in a rectangle triangle	6x4 mm	fill of room, A94, q433, Fs206
Mozan	MZ99 BP51 S2_2	2100-2000	2,1	0,7				trigonometry in a rectangle triangle	4x6 mm	fill of room, A94, q433, Fs206
Mozan	MZ99 BP51 S3_2	2100-2000	3,0	6,1				trigonometry in a rectangle triangle	7x8 mm	fill of room, A94, q433, Fs206
Mozan	MZ99 BP51 S4_2	2100-2000	4,9	5,0				trigonometry in a rectangle triangle	8x4 mm	fill of room, A94, q433, Fs206
Mozan	MZ99 BP51 S5_2	2100-2000	4,0	0,8				trigonometry in a rectangle triangle	6x3 mm	fill of room, A94, q433, Fs206
Mozan	MZ99 BP51b	2100-2000			0,56	7				fill of room, A94, q433, Fs206
Mozan	MZ99 BP51c	2100-2000			0,46	7				fill of room, A94, q433, Fs206
Mozan	MZ99_BP51b_3	2100-2000	1,2	2,0				trigonometry in an isocele triangle	6x8 mm	fill of room, A94, q433, Fs206
Mozan	MZ99_BP51a_3	2100-2000	1,8	1,5	0,37	6	24	trigonometry in an isocele triangle	4x6 mm	fill of room, A94, q433, Fs206
Mozan	MZ99 BP52_2	2100-2000	2,9	1,2				trigonometry in a rectangle triangle		fill of room, A94, q423, Fs206
Mozan	MZ99 BP52a_2	2100-2000	7,0	31,9				trigonometry in a rectangle triangle		fill of room, A94, q423, Fs206
Mozan	MZ01_q0288b_3	2100-2000	3,6	3,4	0,99	2	18	trigonometry in an isocele triangle	4x6 mm	pit fill, A63, q288, Fs1160
Mozan	MZ01_q0288c_3	2100-2000	7,1	5,7	1,11	1	32	trigonometry in a rectangle triangle	4x4 mm	pit fill, A63, q288, Fs1160
Mozan	MZ01_q1203_3	2100-2000	1,5	0,5	0,48	9	15	trigonometry in an isocele triangle	7x11 mm	pit fill, A73, q1203, Fs1351
Mozan	MZ01_q1203b_3	2100-2000	1,2	0,5	0,46	8	13	trigonometry in an isocele triangle	7x13 mm	pit fill, A73, q1203, Fs1351
Mozan	MZ01_q1203e_3	2100-2000	1,3	0,3	0,42	8	15	trigonometry in an isocele triangle	7x13 mm	pit fill, A73, q1203, Fs1351
Mozan	MZ01_q1203c_3	2100-2000	1,2	0,1				circle tool	12x12mm	pit fill, A73, q1203, Fs1351
Mozan	MZ01_q1203d_3	2100-2000	0,9	0,1				circle tool	9x9 mm	pit fill, A73, q1203, Fs1351
Mozan	MZ01_BP25_q0784c_3	2100-2000	2,2	3,0				trigonometry in a rectangle triangle	4x6 mm	pit fill, A73, q784, Fs1351
Mozan	MZ01_BP25_q0784a_3	2100-2000	3,0	19,8				trigonometry in an isocele triangle	5x6 mm	pit fill, A73, q784, Fs1351
Mozan	MZ01 BP25_3	2100-2000	3,2	15,3				trigonometry in a rectangle triangle		pit fill, A73, q784, Fs1351
Mozan	MZ01_BP56_3	2100-2000	0,8	0,6	0,28	5	15	trigonometry in an isocele triangle	2x5 mm	fill, A65, q2282, Fs1898
Mozan	MZ01 BP09 S2_2	2100-2000	3,5	1,9				trigonometry in a rectangle triangle	5x3 mm	pit fill, A63, q322, Fs1160
Mozan	MZ01 BP18 S1_2	2100-2000	6,0	12,9				trigonometry in a rectangle triangle	6x5 mm	dump, A64, q576, Fs1308
Mozan	MZ01 BP18 S2_2	2100-2000	7,4	16,5				trigonometry in a rectangle triangle	4x5 mm	dump, A64, q576, Fs1308
Mozan	MZ01 q2284 S1_2	2100-2000	1,8	4,0				trigonometry in a rectangle triangle	4x8 mm	secondary fill, A65, q2384, Fs1898
Mozan	MZ01 BP33 S1_2	2100-2000	36,4	27,9				trigonometry in a rectangle triangle	9x6 mm	fill in courtyard, A63, q1043, Fs1441
Mozan	MZ01 BP33 S2_2	2100-2000	45,7	35,7				trigonometry in a rectangle triangle	12x13 mm	fill in courtyard, A63, q1043, Fs1441
Mozan	MZ01 BP33 S3_2	2100-2000	13,7	49,0				trigonometry in a rectangle triangle	11x8 mm	fill in courtyard, A63, q1043, Fs1441
Mozan	MZ01 q2935 Fs 1889 S2_1	2100-2000	4,4	3,9				trigonometry in a rectangle triangle	6x6 mm	pit fill, A95, q2935, Fs1889
Mozan	MZ00_q1077_3	2100-2000	5,4	21,6	0,68	7	40	trigonometry in a rectangle triangle	7x5 mm	pit fill, A113, q1077, Fs801
Mozan	MZ00_q1077b_3	2100-2000	6,4	25,2	0,45	6	72	trigonometry in a rectangle triangle	4x6 mm	pit fill, A113, q1077, Fs801
Mozan	MZ99 BP52 S1_2	2100-2000	3,5	6,5				trigonometry in a rectangle triangle	5x4 mm	fill of room, A94, q423, Fs206
Mozan	MZ01_BP33d_3	2100-2000	7,6	14,7	0,34	10	111	trigonometry in an isocele triangle	7x6 mm	fill in courtyard, A63, q1043, Fs1441
Mozan	MZ01_BP33e_3	2100-2000	86,5	1016,9	0,59	10	729	trigonometry in an isocele triangle	15x11 mm	fill in courtyard, A63, q1043, Fs1441
Mozan	MZ01_BP33_3	2100-2000	6,4	15,5	0,34	16	95	trigonometry in an isocele triangle	7x5 mm	fill in courtyard, A63, q1043, Fs1441
Mozan	MZ01_BP33g_3	2100-2000	33,0	314,4	0,37	8	444	trigonometry in an isocele triangle	5x7 mm	fill in courtyard, A63, q1043, Fs1441
Mozan	MZ01_BP33h_3	2100-2000	4,2	1,6	0,30	14	71	trigonometry in an isocele triangle	5x3 mm	fill in courtyard, A63, q1043, Fs1441
Mozan	MZ01_BP33j_3	2100-2000	5,7	5,9	0,31	7	93	trigonometry in an isocele triangle	4x5 mm	fill in courtyard, A63, q1043, Fs1441
Mozan	MZ01_BP33b_3	2100-2000	25,8	150,0	0,44	8	292	trigonometry in a rectangle triangle	8x11 mm	fill in courtyard, A63, q1043, Fs1441
Mozan	MZ01_BP33a_3	2100-2000	4,8	10,2	0,34	9	71	trigonometry in a rectangle triangle	7x8 mm	fill in courtyard, A63, q1043, Fs1441
Mozan	MZ01_BP33i_3	2100-2000	23,5	180,7	0,29	12	409	trigonometry in a rectangle triangle	6x5 mm	fill in courtyard, A63, q1043, Fs1441
Mozan	MP01_BP33k_3	2100-2000	2,9	7,1				trigonometry in a rectangle triangle		fill in courtyard, A63, q1043, Fs1441
Mozan	MZ01_BP61_3	2000-1550	2,3	1,8	0,28	9	41	trigonometry in an isocele triangle	4x3 mm	pit fill, A79, q2551. Fs2043
Mozan	MZ01_q493a_3	2000-1550	3,5	2,7	0,52	8	34	trigonometry in an isocele triangle	6x6 mm	pisé fundament, A84, q494, Fs1070
Mozan	MZ01_q493b_3	2000-1550	5,5	6,6				trigonometry in an isocele triangle	5x10 mm	pisé fundament, A84, q494, Fs1070
Mozan	MZ01_q493c_3	2000-1550	2,4	1,2	0,52	4	23	trigonometry in an isocele triangle	4x8 mm	pisé fundament, A84, q494, Fs1070
Mozan	MZ00_q0343_3	2000-1550	2,0	1,0	2,36	1	4	trigonometry in an isocele triangle	4x3 mm	
Mozan	MZ01_q1586_3	2000-1550	4,3	4,9	0,85	8	26	trigonometry in an isocele triangle	9x10 mm	brickfall, A78, q1586, Fs1145
Mozan	MZ01_q1586b_3	2000-1550	1,8	1,2	0,65	3	14	trigonometry in an isocele triangle	4x4 mm	brickfall, A78, q1586, Fs1145
Mozan	MZ00_q0869d_3	2000-1550	10,9	54,2	0,50	8	108	trigonometry in an isocele triangle	6x6 mm	pit fill, A63/A64, q869, Fs746
Mozan	MZ00_q0869b_3	2000-1550	9,3	8,0	0,52	6	89	trigonometry in an isocele triangle	6x5 mm	pit fill, A63/A64, q869, Fs746
Mozan	MZ99_q0764_3	2000-1550	17,4	15,4	0,92	4	95	trigonometry in an isocele triangle	5x11 mm	fill in room, A64/A74, q764, Fs351
Mozan	MZ01_q606b_3	2000-1550	12,6	46,5	0,37	14	172	trigonometry in an isocele triangle	11x5 mm	fill in courtyards, A75, q606, Fs987
Mozan	MZ01_q606e_3	2000-1550	5,0	10,2				trigonometry in an isocele triangle		fill in courtyards, A75, q606, Fs987
Mozan	MZ01_q1484a_3	2000-1550	17,8	29,0	0,46	12	192	trigonometry in an isocele triangle	7x6 mm	secondary accumulation, A75, q1484, Fs1623
Mozan	MZ01_q1484b_3	2000-1550	9,6	7,9	0,56	13	86	trigonometry in an isocele triangle	11x8 mm	secondary accumulation, A75, q1484, Fs1623
Mozan	MZ00_q1484c_3	2000-1550	0,9	0,0				trigonometry in an isocele triangle	4x6 mm	secondary accumulation, A75, q1484, Fs1623
Mozan	MZ01_q1054_3	2000-1550	0,7	0,1				trigonometry in an isocele triangle	10x5 mm	
Mozan	MZ00_q1054b_3	2000-1550	0,6	0,5	1,82	1	2	trigonometry in an isocele triangle	10x10 mm	
Mozan	MZ99 BP46 S1_2	2000-1550	5,1	3,6				trigonometry in a rectangle triangle	7x4 mm	refuse dump, A94, i745, Fs320
Mozan	MZ99 BP46 S2_2	2000-1550	5,6	2,7				trigonometry in a rectangle triangle	3x4 mm	refuse dump, A94, i745, Fs320
Mozan	MZ99 BP46 S3_2	2000-1550	3,2	7,4				trigonometry in a rectangle triangle	6x3 mm	refuse dump, A94, i745, Fs320
Mozan	MZ99 BP46 S4_2	2000-1550	5,2	0,3				trigonometry in a rectangle triangle	7x3mm	refuse dump, A94, i745, Fs320
Mozan	MZ00_q0082_3	2000-1550	12,4	12,7	0,42	12	148	trigonometry in a rectangle triangle		dump/fill of courtyard, A93/A94, q82, Fs414
Mozan	MZ00_q0261_3	2000-1550	48,2	168,4	0,78	6	309	trigonometry in a rectangle triangle	6x6 mm	brick installation in room, A93, q261, Fs417
Mozan	MZ00 q1296 BP35 Querc. S1_2	2000-1550	4,0	5,4				trigonometry in a rectangle triangle	6x3 mm	fill in courtyard, A75, q1296, Fs904
Mozan	MZ00 q1296 BP35 Querc. S2_2	2000-1550	2,5	1,7				trigonometry in a rectangle triangle	5x5 mm	fill in courtyard, A75, q1296, Fs904
Mozan	MZ00 q1296 BP35 Querc. S3_2	2000-1550	7,1	2,2				trigonometry in a rectangle triangle	4x3 mm	fill in courtyard, A75, q1296, Fs904
Mozan	MZ00 BP33 12993 S1_2	2000-1550	6,3	6,3				trigonometry in a rectangle triangle	10x8 mm	fill in courtyard, A75, q1293, Fs904
Mozan	MZ00 BP33 12993 S2_2	2000-1550	5,9	5,4				trigonometry in a rectangle triangle	15x7 mm	fill in courtyard, A75, q1293, Fs904
Mozan	MZ00 BP33 q1293	2000-1550			0,67	9				fill in courtyard, A75, q1293, Fs904
Mozan	MZ00_BP33_q1293_3	2000-1550	6,4	13,6	0,62	2	52	trigonometry in an isocele triangle	5x3 mm	fill in courtyard, A75, q1293, Fs904
Mozan	MZ99 BP55 S1_2	2000-1550	3,7	8,3				trigonometry in a rectangle triangle	4x4 mm	wall fundament, A84, q505, Fs206
Mozan	MZ00 - q1296 BP35b	2000-1550			0,18	14				pit fill in open area, A75, q1296, Fs904
Mozan	MZ00 - q1296 BP35c	2000-1550			0,17	14				pit fill in open area, A75, q1296, Fs904
Mozan	MZ00_BP35_q1296_3	2000-1550	3,2	1,1	0,19	18	84	trigonometry in an isocele triangle	5x4 mm	fill of courtyard, A75, q1296, Fs904
Mozan	MZ 00_q1296 BP35c_2	2000-1550	3,5	5,7				trigonometry in a rectangle triangle		fill of courtyard, A75, q1296, Fs904
Mozan	MZ99_q797a_3	2000-1550	1,7	2,6	0,37	5	22	trigonometry in an isocele triangle	3x2 mm	grave 4, A94, q797, Fs279
Mozan	MZ99_q797b_3	2000-1550	2,2	2,2	1,34	2	8	trigonometry in an isocele triangle	7x8 mm	grave 4, A94, q797, Fs279
Mozan	MZ00 BP32 S1_2	2400-1800	11,1	30,1				trigonometry in a rectangle triangle	11x10 mm	fill, A85, q1265, Fs804
Mozan	MZ00 BP32 S2_2	2400-1800	9,5	9,6				trigonometry in a rectangle triangle	10x9 mm	fill, A85, q1265, Fs804
Mozan	MZ00_BP32_q1265_3	2400-1800	7,6	15,2	0,86	7	44	trigonometry in a rectangle triangle	7x4 mm	fill, A85, q1265, Fs804
Mozan	MZ00_BP32_3	2400-1800	9,6	22,3				trigonometry in an isocele triangle	8x5 mm	fill, A85, q1265, Fs804
Mozan	MZ00_BP32e_3	2400-1800	13,1	73,0				trigonometry in an isocele triangle		fill, A85, q1265, Fs804
Mozan	MZ00_q0651a_3	2300-1550	96,9	257,4	1,92	1	252	trigonometry in an isocele triangle	7x10 mm	A84, q651, Fs314
Mozan	MZ00_q0651b_3	2300-1550	3,7	3,1	0,76	4	24	trigonometry in an isocele triangle	6x6 mm	A84, q651, Fs314
Mozan	MZ00_q0952_3	2300-1800	5,2	26,7	2,33	3	11	trigonometry in an isocele triangle	10x5 mm	A65, q952, Fs553
Mozan	MZ99 BP74 S1_2	2300-1550	7,3	3,4				trigonometry in a rectangle triangle	6x5 mm	A85, q790, Fs353
Mozan	MZ99 BP74 S2_2	2300-1550	6,8	16,5				trigonometry in a rectangle triangle	9x8 mm	A85, q790, Fs353
Mozan	MZ99 BP74 S3_2	2300-1550	5,0	4,3				trigonometry in a rectangle triangle	3x4 mm	A85, q790, Fs353
Mozan	MZ99_BP74_3	2300-1550	6,5	15,1	0,58	6	56	trigonometry in an isocele triangle	4x4 mm	A85, q790, Fs353
Mozan	MZ99 BP63 S1_2	2100-1550	3,8	12,4				trigonometry in a rectangle triangle	4x4 mm	pit fill, A63, q696, Fs283

Mozan	MZ99 BP63 S2_2	2100-1550	4,9	12,9				trigonometry in a rectangle triangle	3x4 mm	pit fill, A63, q696, Fs283
Mozan	MZ01 BP45 S1_2	2300-2000	1,6	1,5				trigonometry in a rectangle triangle	3x6 mm	pit fill, A74, q1677, Fs1776
Mozan	MZ01_BP84_3	2600-1550	2,0	1,1	0,36	2	28	trigonometry in a rectangle triangle	5x5 mm	
Mozan	MZ01_q2867a_3	2600-1550	5,1	13,5	0,87	3	29	trigonometry in an isocele triangle	4x6 mm	
Mozan	MZ01_q2934_3	2600-1550	1,1	0,5	0,36	7	16	trigonometry in a rectangle triangle	4x3 mm	
Jerablus	JT98 C156_3	3500-3000	4,1	21,2				trigonometry in a rectangle triangle		floor of building, Area III, Unit 2192
Jerablus	JT96_C91_1512a_3	3000-2800	2,8	2,4	0,39	14	36	trigonometry in an isocele triangle	7x4 mm	pit fill , Area III, Unit 1512
Jerablus	JT98 C131b_2	3000-2800	2,4	2,7				trigonometry in a rectangle triangle		pit fill, Area III, Unit 2028
Jerablus	JT98 C131a Unit III 2028	3000-2800			0,21	8				pit fill, Area III, Unit 2028
Jerablus	JT00 C219	3000-2800			0,91	5				occupation deposit, Area IIIA, Unit 2757
Jerablus	JT96_C91_1512b_3	3000-2800	8,0	22,8	0,43	12	93	trigonometry in a rectangle triangle	7x4 mm	fill, Area I, Unit 1563
Jerablus	JT96_C134[1563]a_3	2800-2250	3,0	3,1				trigonometry in an isocele triangle	6x3 mm	fill, Area I, Unit 1563
Jerablus	JT96_C134[1563]c_3	2800-2250	2,1	3,6	1,33	2	8	trigonometry in an isocele triangle	7x4 mm	fill, Area I, Unit 1563
Jerablus	JT96_C134[1563]d_3	2800-2250	4,5	7,4	0,36	5	62	trigonometry in an isocele triangle	7x4 mm	fill, Area I, Unit 1563
Jerablus	JT96_C134[1563]e_3	2800-2250	4,0	14,0	0,45	6	45	trigonometry in an isocele triangle	5x3 mm	fill, Area I, Unit 1563
Jerablus	JT96_C134[1563]h_3	2800-2250	2,8	1,9	0,88	3	16	trigonometry in an isocele triangle	5x5 mm	fill, Area I, Unit 1563
Jerablus	JT96_C134[1563]i_3	2800-2250	2,5	0,8	1,31	1	9	trigonometry in an isocele triangle	6x3 mm	fill, Area I, Unit 1563
Jerablus	JT96_C134[1563]b_3	2800-2250	1,0	0,4				trigonometry in a rectangle triangle	6x4 mm	fill, Area I, Unit 1563
Jerablus	JT96_C134[1563]f_3	2800-2250	4,4	3,0				trigonometry in a rectangle triangle	5x3 mm	fill, Area I, Unit 1563
Jerablus	JT96_C134[1563]g_3	2800-2250	5,7	10,0				trigonometry in a rectangle triangle	6x3 mm	fill, Area I, Unit 1563
Jerablus	JT93 C11 235	2800-2250			0,24	19				building fill, Area IIIC, Unit 235
Jerablus	JT94 C14	2800-2250			0,36	6				floor, IIIC, Unit 342
Jerablus	JT94 C14a	2800-2250			0,55	8				floor, IIIC, Unit 342
Jerablus	JT94 C14b	2800-2250			0,35	6				floor, IIIC, Unit 342
Jerablus	JT95 C61 Awl 989	2800-2250			0,28	12				indetermined, Area I, Unit 989
Jerablus	JT98 C132a	2800-2250			0,55	5				fill, Area I, Unit 1563
Jerablus	JT98 C132c	2800-2250			0,57	5				fill, Area I, Unit 1563
Jerablus	JT00 C227 3096 a_2	2800-2250	12,3	5,2				trigonometry in a rectangle triangle		occupation deposit, Area I, Unit 3096
Jerablus	JT00 C227 3096 b_2	2800-2250	2,6	0,0				trigonometry in a rectangle triangle		occupation deposit, Area I, Unit 3096
Jerablus	JT00 C227 3096 d _3	2800-2250	3,4	12,4				trigonometry in a rectangle triangle		occupation deposit, Area I, Unit 3096